

Early detection of the breast cancer using infrared technology – A comprehensive review

Aigerim Mashekova^{a,*}, Yong Zhao^a, Eddie Y.K. Ng^b, Vasilios Zarikas^a, Sai Cheong Fok^a, Olzhas Mukhmetov^a

^a Nazarbayev University, School of Engineering and Digital Sciences, Nur-Sultan, Kazakhstan

^b Nanyang Technological University, School of Mechanical and Aerospace Engineering, Singapore

ARTICLE INFO

Keywords:

Thermography
Breast cancer
Numerical modeling
Reverse modeling
Artificial intelligence
Machine learning

ABSTRACT

Breast cancer is one of the most common and deadly diseases in women, which can also affect men. Early detection and treatment of this disease can increase the chances of cure. Currently, there are many different approaches to breast cancer screening, each of which has its own advantages and disadvantages. Thermography is one of those breast cancer screening methods that is considered safe and non-invasive. The approach with new image processing and intelligent classification techniques has gained renewed interest. The non-contact technology, which is relatively inexpensive, has great potential for integration with the Internet for early detection of breast cancer through mass screening and subsequent continuous monitoring of suspected patients. This paper presents a comprehensive review of previous studies conducted at the intersection of thermography, numerical simulation, and artificial intelligence that can improve early detection of breast cancer.

1. Introduction

Cancer is a term used to describe a number of diseases associated with uncontrolled cell mutations resulting from tumor enlargement [1]. Tumors commonly occur in organs such as the skin, lungs, prostate, breast, and pancreas. There are no exact factors that influence the spread of such a disease, but most experts agree that an unhealthy lifestyle, alcohol consumption, smoking, ultraviolet radiation, the influence of carcinogens, age and a genetic predisposition are some of the most common causes for the development of tumors [2,3].

Breast cancer is one of the most common types of cancer. According to the World Health Organization (WHO), 2.3 million new cases of breast cancer was detected in women worldwide in 2020. In the past five years (2016–2020), there were 7.8 million women diagnosed with breast cancer, making it the most common cancer worldwide. WHO reports that the number of deaths caused by breast cancer during this period is 685,000. This number is less than the number of deaths due to other cancers such as lung (1.8 million deaths), liver (830 thousand

deaths) and stomach (769 thousand deaths) [4,5]. This shows that breast cancer is treatable. Currently, breast tumors are diagnosed based on the stages of tumor development, which can be classified based on tumor diameter or spread to nearby lymph nodes [4]. Accurate and early diagnosis plays an important role in the successful treatment of the disease, which has generated a great deal of interest [5,6].

Most studies of breast cancer diagnosis have focused on mammography, ultrasound, and Magnetic Resonance Imaging (MRI). These approaches are recognized as the gold standard. However, their limitations, such as lack of access to cancer detection in rural and remote areas, have led to the development of alternative technologies: electronic palpation, electrical impedance scanning (EIS), and thermal imaging (thermography) [1]. This paper focuses on thermography as it is one of the most cost-effective, non-invasive, radiation-free and prospective techniques.

Thermography (also called infrared imaging) uses infrared (IR) cameras to record the temperature profiles of the breast. The presence of a tumor can thus be determined by the temperature distribution on the

Abbreviations: AI, artificial intelligence; ANN, artificial neural network; BN, Bayesian network; CAD, computer-aided diagnosis; CNN, convolutional neural network; DIT, dynamic infrared thermography; FDA, food and drug administration; GA, genetic algorithm; IR, infrared; IBT, infrared breast thermography; ML, machine learning; MLT, machine learning technologies; NN, neural network; ROI, region of interest; SVM, support vector machine.

* Corresponding author.

E-mail addresses: aigerim.mashekova@nu.edu.kz (A. Mashekova), yong.zhao@nu.edu.kz (Y. Zhao), MYKNG@ntu.edu.sg (E.Y.K. Ng), vasileious.zarikas@nu.edu.kz (V. Zarikas), scfokky@yahoo.com.au (S.C. Fok), olzhas.mukhmetov@nu.edu.kz (O. Mukhmetov).

<https://doi.org/10.1016/j.tsep.2021.101142>

Received 23 August 2020; Received in revised form 8 August 2021; Accepted 12 November 2021

Available online 20 November 2021

2451-9049/© 2021 The Author(s).

Published by Elsevier Ltd.

This is an open access article under the CC BY-NC-ND license

(<http://creativecommons.org/licenses/by-nc-nd/4.0/>).

breast surface [7–9]. The main principle of IR image diagnosis is that the unregulated growth of cells generates a higher metabolic rate and requires more blood flow than the surrounding tissue. The additional heat generated is delivered to the tissue surrounding the tumor, causing a temperature spike on the breast surface. This temperature spike is observed using IR imaging to detect the tumor [7–9].

Diagnosis of breast cancer using thermography is based on identification of specific features of breast heat patterns over time. The most common features include: 1) highly asymmetric temperature distributions between the left and right breasts (i.e., based on the assumption that one is healthy and the other is not); 2) localized hot spots indicative of abnormalities; 3) changes in hypothermic vascular patterns due to tumor growth; 4) variation in heat patterns in the areolar and periareolar regions [10–12].

It is important that the breast size and geometry, as well as physiological conditions such as menstruation, stress and anxiety, hormone use (contraceptives), pregnancy, and lactation be considered in decision making, as sometimes a temperature difference of 2 °C between the cooler and warmer regions and between asymmetric areas of two breasts may be considered normal, while a difference of 1 °C to 2.5 °C may be considered suspicious [8,13,14].

The following sections discuss breast cancer using IR imaging and computer technology.

2. Breast thermography

The fundamentals of thermography come from previous studies by Hardy [15,16,17], Hardy and Muschenheim [18,19], Clark, Vinegar and Hardy [20], Hardy, Hammel and Murgatroyd [21], Derksen, Monahan and Lawes [22], Mitchell [23], Quinn [24], Watmough [25], Steketee [26], Quinn and Compton [27], Pratt [28], and Andersen and Parrish [29], who concluded that IR cameras can provide reliable measurements of actual temperatures. They found that the emissivity of the skin is about 0.989 ± 0.01 and does not depend on the wavelength, while the relationship between spectral radiance and wavelength can be described by Planck's radiation law, where the intensity of electromagnetic radiation (B) is a function of the wavelength (λ) and the temperature of the object (T), as described by the following equation:

$$B_{\lambda}(\lambda, T) = \frac{2hc^2}{\lambda^5} (e^{\frac{hc}{\lambda T}} - 1)^{-1} \quad (1)$$

where $B(\lambda, T)$ – radiation power; h – the Planck constant, c_s – the speed of light in vacuum, and k – the Boltzmann constant.

Thermography was first used to diagnose breast cancer in 1956 [30]. Further studies by Lawson and Chughtai showed that the temperature difference between healthy and diseased breast in the same area is about 20 °C [31]. The same results were obtained by Gautherie [32] in 1980, who used a fine needle thermocouple to measure the temperature inside the breast with malignant tumor. Other studies [2,12,14,31,33–42] gave similar results, showing that the presence of the tumor in the breast leads to a higher temperature, which shows up as a hotspot on the thermogram. In 1982, thermography was approved as an additional tool to mammography for breast cancer diagnosis in the United States of America.

Further development of infrared thermography for breast tumor detection has had some successes and drawbacks. A clinical study by Gamagami [43] reported that 15% of nonpalpable carcinomas went undetected by mammography but were detected by IR thermography. Gautherie and Gross [12,44] studied 1245 patients with abnormal IR image profiles and found that 35% of patients with abnormal thermograms developed cancer within the next 5 years. They noted that IR imaging may be useful for early detection of breast cancer and fast-growing neoplasms. However, the approach was unable to distinguish the cancerous region of the breast from areas of inflammation. In addition, the false-positive results for breast cancer were high [32]. The

rate of correct positive diagnoses was only 41%. This was attributed to both the measurement procedure and the equipment. Most clinicians were neither familiar with nor adequately trained in the use of IR cameras, and measurement standards were lacking [32]. In addition, poor camera resolution and scan time compromised the usefulness of the approach at the time. Chen et al [35] stated that the specification of the cameras was limited as the typical resolution was low and the scan time was 4 s. Such a specification was not suitable for detecting deep tumors, only shallow tumors could be diagnosed. This is because the temperature pattern of the healthy breast and the deep tumours can be very subtle. These problems hinder the popularity of IR thermography as a method for early detection of breast cancer [12,44–46].

In the 2000s, IR cameras significantly improved their performance, especially when used in conjunction with a blackbody, and nominal accuracy could be varied from 0.1 to 1 °C and a scan time of 0.8 s (Table 1). This improvement in the performance of the cameras allowed deeper tumors to be detected and less pronounced temperature variations to be observed on the breast surface. This also led to the development of breast tumor detection methods such as dynamic infrared thermography (DIT). The method aims to detect the thermal contrast between cancerous and non-cancerous regions during rewarming of the breast after the application of cold stress. The principle is based on the fact that the temperature patterns of the cancerous region in the breast remain the same, while the healthy regions are affected by cold stress. Similarly, the cancerous breast under cold stress exhibits different temperature patterns than a healthy breast. In the studies conducted by Usuki et al [47], Cockburn [48] and Mooibroek et al [49], it was observed that tumors produce a chemical mediator under thermal stress. This chemical dilates subcutaneous vessels and enhances the contrast of temperature differences between the tumor and the environment [50]. The magnitude of the response to thermal stress can vary depending on tumor size. The effects of cold stress on different tumor sizes remain to be thoroughly investigated. According to Gullino [51], the response of tumor vessels to cold stress may be insignificant in deeper tumors.

One of the most important studies in the field of DIT was conducted by Ohashi and Uchida [52], who studied 728 cases of breast cancer using thermograms from steady-state and dynamic infrared images. During the experiments, the ambient temperature was maintained at 21 °C, and a fan was used for 2 min for DIT. The diagnostic accuracy of steady-state thermography was 54%, while the diagnostic accuracy of DIT was 82%, see [52]. To increase the diagnostic accuracy of melanoma a similar DIT method was developed in [53]. In this work, it was emphasized that the proper performance of steady-state thermography requires strict requirements for the environmental conditions in the room, as well as adequate time for the patient to adjust to the room temperature. DIT does not require such stringent room conditions and is both faster and more effective in creating thermal contrast between the tumor and surrounding healthy tissue. To further improve the performance of DIT with modern IR detectors, Ng [45] suggested minimizing the sources of IR interference. Minimizing unwanted interference can be achieved by using a smooth, non-reflective background, covering IR reflective surfaces, and blocking sunlight through windows and incandescent or halogen light sources. The major disadvantage of DIT is that there is no standardized and systematic approach. Accurate and meaningful results depend on the size and depth of the tumor. Another major problem of DIT is the discomfort of the patient during the application of cold stress, as the cooling time can range from 2 to 6 min at temperatures below 15 °C [54,55]. The results of various studies show a very high variation in the accuracy of dynamic thermography, so that it is not preferred in practice despite its high accuracy.

Many researchers have investigated the prognostic aspects of IR thermography in the detection of breast cancer. Isard et al [37,56] conducted a study of 10,000 breast thermograms over four years before recommending thermography as a complementary tool to mammography rather than a stand-alone tool for breast cancer detection. It was found that of the 1000 cases that underwent both thermography and

Table 1

List of selected infrared cameras for medical applications.

	Measuring range	Resolution (pixels)	Thermal sensitivity	Spectral range	Temperature measurement accuracy	Application	Function
Micro-Epsilon	−20 °C to 100 °C	382×288	40 mK	7.5–13 μm		fever screening;	thermal imaging,
IRTIS 2000	−60 °C – +300 °C (+1700 °C)	320 (640) ×240 (480)	0.05° C (0.02° C)	3–5 (8–12) μm	±1% or ± 1 °C	medical	measuring thermal imaging
Fluke Ti480 PRO Infrared Camera	≤−20 °C to 1000 °C	640×480	50 mK	7.5 μm to 14 μm (long wave)	±2 °C or 2% (at 25 °C nominal, whichever is greater)	universal	thermal imaging
Hikvision CA-DS- 2TE127-G4A	5 °C –50 °C	160×120	Less than 40 mK	8 – 14 μm	± 0.1 °C	medical	thermal imaging
Flir T560-EST	down to −40 °C	640×480	less than 40 mK @ 30 °C (86°F)	7.5 – 14 μm	±1°C/±1%	universal	thermal imaging

mammography, 45% of the thermograms were found to be abnormal and 21.4% were eventually confirmed as cancerous by mammography. In another study of 70 patients followed up between 6 and 13 years, Isard concluded that thermography could be a prognostic indicator of survival. Gautherie and Gros [12] found that patients with abnormal

thermograms had a higher risk of later developing breast cancer. Another study [57] found that thermography results were strongly correlated with prognostic indicators of tumor growth, such as tumor ferritin concentration, the proportion of cells undergoing DNA synthesis and proliferating, and expression of the proliferation-associated tumor

Table 2

Main studies and its mathematical models.

Authors	Equation	Meaning
Pennes, 1948 [50]	$\rho_{ti}c_{ti}\frac{\partial T}{\partial t} = \nabla \cdot (k_{ti}\nabla T) - \omega_b c_b (T - T_{art}) + q_m$ where ρ_{ti} – tissue density; c_{ti} – tissue specific heat; k_{ti} – tissue thermal conductivity; c_b – blood specific heat; T – temperature; q_m – heat generations due to metabolism; ω_b – blood perfusion rate; T_{art} – arterial blood temperature; t_i , b , art – subscripts indicating tissue, blood, artery, respectively	Frequently used equation based on Fourier's law considering thermal energy equilibrium: equalisation of temperature in tissue depending on external and internal heat sources.
Mitchell and Myers, 1968 [36]	(1) $mc\frac{dT_{art}}{dx} + (UA)', (T_{art} - T_v) + (UA)'_{art}(T_{art} - T_{\infty}) = 0$ $-mc\frac{dT_v}{dx} + (UA)', (T_v - T_{art}) + (UA)'_v(T_v - T_{\infty}) = 0$ $x = 0 : T_{art} = T_0; x = L : T_{art} = T_v$ U – thermal conductance; A' – heat transfer area per length; ΔT – temperature difference causing the heat flow; T_v – vein blood temperature; v – subscripts to indicate vein	One of the first equations of the discrete vessel approach, where the first equation describes the arterial flow, the second equation gives the venous flow, and the last equation represents the temperature boundary conditions
Keller and Seiler, 1971 [39]	$k_{ti}\frac{d^2 T}{dx^2} + (h_a + c_b g)(T_{art} - T) + h_a(T_v - T) + q_m = 0$ $[(m_{art})_0 - \int_0^x g dx]c_h \frac{dT_{art}}{dx} + h_a(T_{art} - T) = 0$ $[(m_{art})_0 - \int_0^x g dx]c_h \frac{dT_v}{dx} + (h_a + c_b g)(T - T_v) = 0$ with the following boundary conditions $x = 0, T = T_{art} = T_b; x = \delta, T = T_v = T_s$ where x – length in the direction of normal to surface, h – average coefficient of heat transfer from vessels to tissues, a – average area for heat transfer per unit volume, c_h – heat capacity, g – capillary perfusion rate, m – blood flow rate, S – thickness of tissue layer; s – subscripts to indicate skin	Extension of the Mitchell and Myers biothermal system of equations by adding the conservation of energy in the surrounding tissues of the veins and capillaries in the area of interest. The influence of the perfusion rate of the capillaries on heat transfer in the subdermal area is included
Wulff, 1974 [61]	$\rho_b c_b \frac{\partial T}{\partial t} = \nabla \cdot (k_{ti}\nabla T) - p_b c_b U_h \cdot \nabla T + q_m,$ where ρ_b – blood density; U_h – metabolic reaction enthalpy	Mathematical model of the equilibrium of blood and tissue temperatures and the value of the metabolic reaction ($p_b c_b U_h \cdot \nabla T$), corresponding to q_m
Chen and Holmes, 1980 [40]	$p_{ti,eff}c_{ti,eff}\frac{\partial T}{\partial t} = \nabla \cdot (k_{ti}\nabla T) + p_b c_b w_b (T_{art} - T) - p_b c_b v \cdot \nabla T + \nabla \cdot k_p \nabla T + q_m,$ where $\rho_{ti,eff} = (1 - \varepsilon_{tp})\rho_a + \varepsilon_{tp}\rho_b c_{ti,eff} = (1 - \varepsilon_{tp})c_{ti} + \varepsilon_{tp}c_b k_{ti,eff} = (1 - \varepsilon_{tp})k_{ti} + \varepsilon_{tp}k_b$ where v – direction of the flow, which is volumetric flow of the unit area, k_p – perfusion conductivity; t_p – subscripts to indicate tissue porosity	Discrete vessel model describes the heat exchange between a single blood vessel and the surrounding tissue
Weinbaum, Jiji, Lemons, 1984–1992 [62–69]	$\rho_b c_b \pi r^2 v \cdot \frac{dT_{art}}{ds} = -q_{art}\rho_b c_b \pi r^2 v \cdot \frac{dT_v}{ds} = -q_v \rho_b c_b \frac{\partial T_{ti}}{\partial t} = \nabla k_{ti} \Delta T_{ti} + \left[n q \rho_b c_b (T_{art} - T_v) - \rho_b c_b n \pi r^2 v \cdot \frac{d(T_{art} - T_v)}{ds} \right] + q_m$ where q_{art} – heat loss from an artery due to heat conduction through its wall; q_v – heat influx into a vein due to heat conduction through its wall; T_{art} and T_v – volumetric mean temperatures inside the blood vessel; r – radius of the vessel; v – the speed of the flow through the artery or vein; n – number of the arteries and veins; q – blood flow velocity per unit surface area of the vessel. Or the simplified version of the Weinbaum, Jiji and Lemons model can also be used: $\rho_{ti}c_{ti}\frac{\partial T_{ti}}{\partial t} = \nabla k_{eff}\nabla T_{ti} + q_m$ where k_{eff} – effective conductivity, which can be defined as: $k_{eff} = k_{ti}[1 + Pe_i V(\xi)]$, where ξ – dimensionless distance, defined as x/L ; L – tissue layer thickness; $V(\xi)$ – dimensionless function of vascular geometry that can be calculated if vascular information is known; Pe_i – Peclet number, which is defined as: $Pe_i = \frac{2\rho_b c_b r_i v_i}{k_b}$ where r – radius of vessel; v_i – blood velocity at the entrance to the tissue.	The first two equations describe heat transfer in the major (thermally significant) arteries and veins. The third equation describes heat transfer in the tissue surrounding the artery-vein pair. The fourth equation is a simplified representation of the first three equations to estimate the temperature distribution in the tissue

antigen Ki-67. Thus, the patients with abnormal thermograms had faster-growing tumors, which could be indicated by the thermograms. The conclusion was based on the results of 100 normal patients, 100 living cancer patients, and 126 deceased cancer patients. In a study by Guidi and Schnitt [58], a strong correlation was found between the number of vessels and further spread of metastatic disease.

In most studies, thermography was recommended as an additional tool to complement mammography. This result was also confirmed in a recent study by Omranipour et al [59] who compared the true-positive rate (TPR), true-negative rate (TNR), positive predictive value (PPV) and negative predictive value (NPV) of thermography and mammography. The results for mammography were: TPR 80.5%, TNR 73.3%, PPV 85.4%, NPV 66.0%; in contrast, the results for thermography were: TPR 81.6%, TNR 57.8%, PPV 78.9%, and NPV 69.7%. These results confirm that thermography can complement, but not replace, mammography in the early detection of breast cancer. The US Food and Drug Administration (FDA) also does not recommend thermography as the sole tool for breast cancer detection, but recommends it as an adjunct tool along with another diagnostic technique [60]. This could be due to the disadvantages of the technique. Thermography is very sensitive to the temperature and comfort of the patient. In addition, the technique is prone to procedural errors, such as incorrect positioning of the breast, inability to eliminate nearby heat sources, and difficulty in maintaining an appropriate distance between the IR camera and the patient. These errors resulted in poor thermal images with occluded areas, especially in large breasts with fatty tissue.

3. Numerical thermal simulation of breast cancer

3.1. Mathematical equations

Heat transfer in living tissues is a complex thermal process consisting of metabolic heat generation, heat conduction, and blood flow. With regard to breast cancer diagnosis, a number of studies have developed mathematical models to describe heat transfer behavior and predict the temperature distribution of breast tissue and the presence of a tumor in the breast. Table 2 shows the main studies and mathematical models of each approach in the studies.

The mathematical equations for biothermy presented in Table 2 can be described using two main approaches: Continuum Models and Discrete Vessel Models. The continuum model is the simplified form of the biothermal equations that describe the effects of blood flow on temperature distribution by considering the average blood supply over the average volume in the area of interest. The continuum approach was used in the work of Pennes [50] and the energy conservation equation of Wulff [61].

The discrete vessel model is a more advanced and sophisticated approach based on biothermal equations that describe the blood flow in each individual vessel in the region of interest. This approach was described in the work of Mitchell and Myers [36], Keller and Seiler [39], Chen and Holmes [40], and Weinbaum-Jiji-Lemons, which included a simplified version of their model [62–69].

The idealized mathematical models of Pennes and Wulff that are often used by scientists neglect effects such as heat transfer between blood and tissue, blood flow, and the size of blood vessels and their position relative to each other. Pennes' equation agrees well with experimental data and is often used to describe the temperature distribution in the area of interest. The more sophisticated discrete vessel model takes into account detailed information about the vascular network and blood flow. The approach takes into account the existence of temperature differences between arteries and veins that are close to each other, and the heat transfer that occurs when they flow in opposite directions. The approach requires a set of biothermal equations that describe the movement of blood in each blood vessel. This also takes into account the opposing flow, which has a significant effect on the equilibrium of heat transfer. As a result, the temperature distributions in the adjacent tissues of

interest can be predicted with higher resolution. In particular, the mathematical model of Weinbaum-Jiji-Lemons can describe the heat transfer in acentric tissues, provided that its assumptions are valid. Anatomical and vascular geometric data are needed to apply the model. The data include the density of the vessels, the size and distance between artery and vein, and the blood flow rate.

Many researchers have used these mathematical models to study the effects of blood flow and blood vessel diameter on temperature distributions. According to Chato et al [41], higher blood flow decreases as the blood vessel becomes smaller, so the heat transfer coefficient can be determined in counterflow. Charny and Levin [70] studied the heat transfer between artery and vein and showed that the thermal equilibrium of the system can be reached at a distance of 43 mm from the main vessels. Furthermore, it was found that the counterflow can lower the temperature of the tissue by 0.5 °C. This work illustrated the applicability of mathematical models. The choice of an appropriate biothermal model should be based on the objectives of the study and the specific biophysical characteristics of the cases.

3.2. Breast geometry involved in simulations

The geometry of the breast is another important factor in the numerical simulations. Many different computational geometries have been used in the thermal simulations, including rectangular, idealized spherical, and realistic geometries of the breast [35,71–73]. Table 3 provides a list of domains found in the literature.

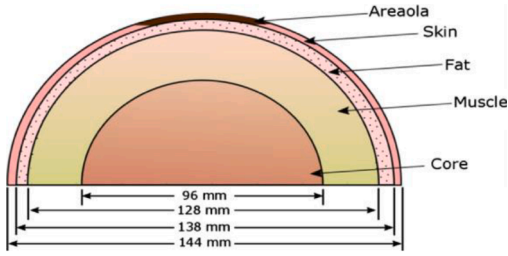
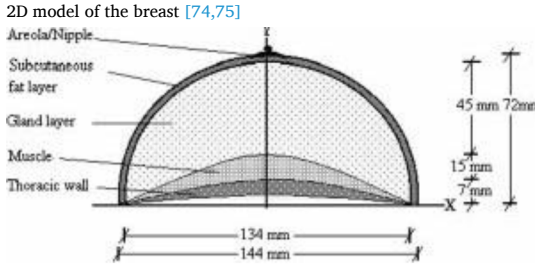
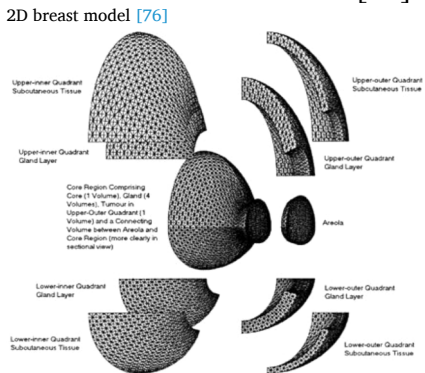
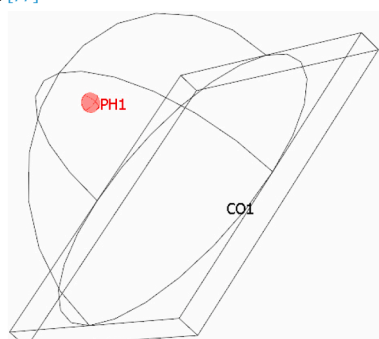
Table 3 lists the studies that used different breast geometries and predictive models to relate temperature distributions to tumor sizes, location, metabolic heat generation, and blood perfusion rates. Four main types of breast geometries were developed in these studies [74–85]: rectangular, hemispherical, deformed hemisphere, and patient-specific.

Osman and Afify [74,75] developed a multilayer 2D breast geometry in 1984. This work was extended in 1988 with a 3D breast geometry to estimate the effect of tumor size and location on breast surface temperature distribution. This model has not been used by other researchers because it leads to high temperature differences in the layers near the surface [86].

Further studies by Ng and Sudharsan [76,77] led to an improvement in both 2D and 3D multilayer breast models. They created flexible 3D models with tissue layers of different thicknesses and divided the geometry into four quadrants to study the temperature differences in the upper outer, lower outer, upper inner, and lower inner segments. This model has been used in many studies to determine the effects of various tumor parameters on thermal distributions.

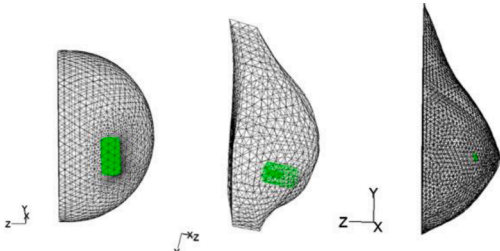
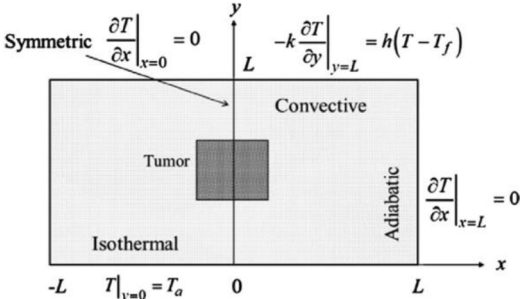
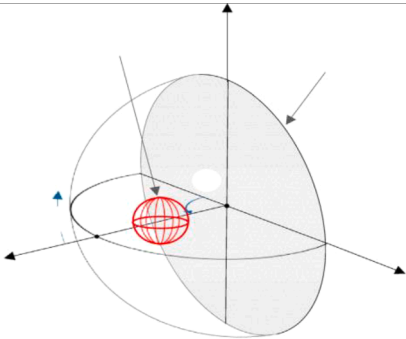
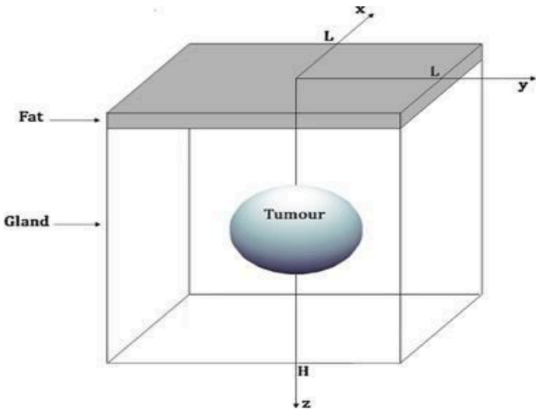
Gonzalez [78] used a hemispherical breast model and added a thick layer of 1.3 cm to simulate the chest wall. The results of the study showed that Finite Element Simulations is able to detect 3 cm tumors located at a depth of 7 cm from the surface. Bezerra et al [79] modeled the breast geometry based on the silicone prostheses. The cylindrical geometry was improved with nodule type, size, depth, and location extracted from a patient's ultrasound examination. The study established the methodology for determining the thermophysical properties of the breast tissue and nodes using the maximum temperature from the temperature profile. In 2013, Das and Mishra [80] used a rectangular single-layer breast model with Pennes' bioheat equation to diagnose a tumor based on the temperature distribution on the surface of the breast. The rectangular model does not reflect the actual shape of the breast, and it was difficult to validate the results with thermograms. As a result, no firm conclusions could be drawn. Later, the authors created a single-layer hemispherical 3D model with a tumor [81] and found that the developed tool can be used to detect not only small tumors near the breast surface, but also large tumors located deep in the breast when there is a significant temperature difference at the breast surface. Amri et al [82] used a rectangular 3D breast model to perform steady-state and transient numerical simulations. Their results showed that the

Table 3
Computational domains.

Study	Breast Geometry	Description
Osman, Afify, 1984; Osman, Afify, 1988 [74,75]	 <p>2D model of the breast [74, 75]</p>	2D and 3D models were developed to estimate the influence of tumor size and location on temperature distributions on the breast surface
Ng, Sudharsan, 2000 [76]	 <p>2D breast model [76]</p>	A 2D breast model was developed to perform an analysis of variance, and a parametric design using the Taguchi method was used
Ng, Sudharsan, 2001 [77]	 <p>3D breast model [77]</p>	The flexible multilayer finite element model was divided into four quadrants. The model was used to study steady-state and time-dependent numerical simulations
Gonzalez, 2007 [78]	 <p>Ideal hemispherical model of the breast consisted of: hemisphere, chest wall, tumors [78]</p>	Perfect hemispherical breast model for studying the required sensitivity of the thermal imaging camera to detect a tumor in the breast at the specified depth
Bezerra et al., 2012 [79]		The breast model was created manually and approximately based on simplified thermogram side views and used to estimate the thermal conductivity and blood flow of the breast tissue

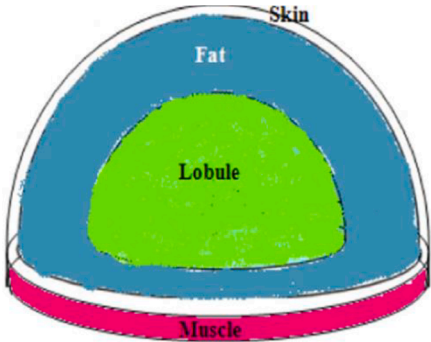
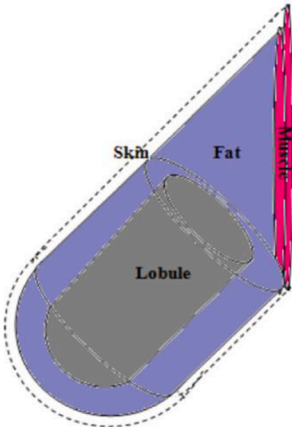
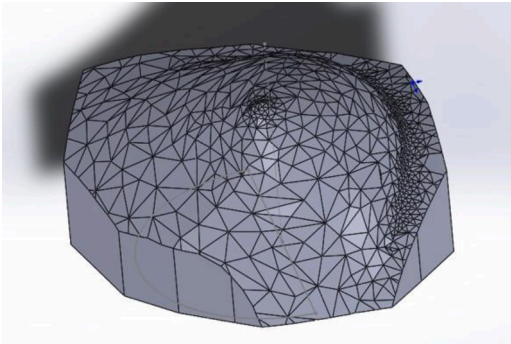
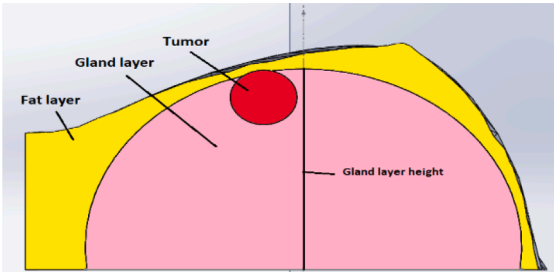
(continued on next page)

Table 3 (continued)

Study	Breast Geometry	Description
		
	<p>Thermogram based 3D breast models [79]</p> <p>Thermogram based 3D breast models [79]</p>	
Das and Mishra, 2013 [80]		The study focused on the evaluation of predictive algorithms, using the temperature distribution on the breast surface to investigate tumor behavior. The study used a proprietary numerical code and Pennes mathematical model
Das, Mishra, 2015 [81]		The breast model used four parameters to define the tumor: size, radial location, and two coordinates of two angular positions
	<p>Idealized 3D breast model [81]</p> <p>Idealized 3D breast model [81]</p>	
Amri et al., 2016 [82]		In the study, steady-state and transient numerical simulations with cold stress were performed to determine the effect of depth on temperature using Pennes' bioheat equation; a simple rectangular 3D breast model was used
	<p>3D rectangular breast model with a spherical tumor inside [82]</p> <p>3D rectangular breast model with a spherical tumor inside [82]</p>	
Hossain, Mohammadi, 2016; Saniei, et al., 2016 [83,84]		The multilayer breast model was used for the idealized hemisphere model and the deformed hemisphere breast model. The model was used to estimate physio-thermo-biological parameters such as depth, size and metabolic rate of tumor

(continued on next page)

Table 3 (continued)

Study	Breast Geometry	Description
	<div><div>a)</div><div>b)</div></div>	<p>Breast model: a) hemisphere breast model, four concentric tissue layers; b) deformed hemisphere breast model, four concentric tissue layers [83]</p> <p>Breast model: a) hemisphere breast model, four concentric tissue layers; b) deformed hemisphere breast model, four concentric tissue layers [83]</p>
Mukhmetov et al., 2018 [73]		<p>Patient-specific breast model created by 3D scanning and used to estimate temperature distribution based on tumor size and depth in the breast. Reverse thermal modelling was also performed to determine specific patient tissue characteristics and tumor size and location</p>
	<p>Patient's specific breast model [73]</p> <p>Patient's specific breast model [73]</p>	
Aitbek et al., 2019 [85]		<p>A multilayer breast model was used to estimate the effect of breast density on tumor detection</p>
	<p>Multilayer breast model [85]</p> <p>Multilayer breast model [85]</p>	

rewarming process after the application of cold stress provides more information about the tumor. However, the main problem with rectangular breast models is that they do not correlate with real breast geometry and its tissue layers. Moreover, such breast geometry used uniform properties for the tissue and tumor, which could not be validated by experiments.

There are many studies based on rectangular and spherical computational domains, but very little literature on the use of personalized breast geometries of patients in numerical studies. Mukhmetov et al [73] created 3D numerical models by scanning a mannequin and real patient breasts. The obtained numerical results were validated by experiments with artificial and human breasts. Aitbek et al [85] improved the patient-specific model by creating different layers inside the breast and estimating the influence of fat on the temperature distribution on the breast surface, thus identifying the tumor inside the breast.

3.3. Forward/direct and inverse simulations for breast cancer detection

Numerical modeling of the tumor in the breast is a complicated procedure, but it is a reliable technique to complement thermography with quantitative assessments. The studies using physical models to predict the temperature distribution on the breast surface and in the breast volume are called forward or direct numerical simulations.

Numerical simulation first requires the creation of a relevant breast geometry (see Section 3.2) with appropriate boundary conditions. Then, the governing mathematical equations (see Section 3.1) are solved numerically in the breast region. Researchers have used various approaches to solve Pennes' equation. Huang et al [87] solved Pennes' bioheat equation analytically for two cases that differed in terms of arterial temperature. In the first case, the arterial temperature was equal to the mean temperature of the vessel, while in the second case, the arterial temperature was constant. Zhang [88] solved the bioheat equation using Lattice Boltzmann Method, which produced a precise temperature distribution. Okajima et al [89] solved the one-dimensional Pennes' bioheat equation and derived two general dimensionless characteristics of bioheat transfer for steady state.

Many studies solved the bioheat equation in different coordinate systems. Gupta et al [90] solved the bioheat equation in spherically symmetric, axisymmetric and Cartesian coordinate systems using Galerkin method. By solving the heat equations in different coordinate systems and considering different breast models, the researchers showed that the location and size of the tumor in the breast have primary effects on the temperature distribution on the breast surface.

Studies such as those in [7,9,54,74–77,82,86,88,91] concluded that the temperature patterns depend on the diameter and depth of the tumor and agreed that small and deep-seated tumors are difficult to detect because the temperature patterns have low contrast in the surface temperature distributions. Das and Mishra [80] investigated the effect of depth on the patterns of temperature distributions by calculating the temperature differences between tumors 12.5 mm and 37.5 mm in diameter at a depth of 12.5 mm. Their results showed surface temperature differences of 0.007 °C and 0.56 °C, respectively. Amri et al [82,91] determined the temperature differences for different tumor sizes from 10 to 30 mm at the same depth of 20 mm. The results showed temperature differences of about 0.2 °C for tumors of 10 mm and 30 mm (Fig. 1), indicating that the size of the tumor does not have much influence at a depth of 20 mm and deeper. Ng and Sudharsan [76,77] reported that tumors deeper than 38 mm have a very low chance of being detected by the IR camera. These results confirm that the depth of the tumor has a much greater impact compared to the tumor diameter. The depths at which tumors were most unlikely to be detected ranged from 20 mm to 30 mm.

Temperature contrast at the surface of the breast can be increased by the application of cold stress. This phenomenon was described in detail by Usuki et al. in [47]. Cold stress may enhance the temperature difference between the healthy and cancerous tissues, thus improving the

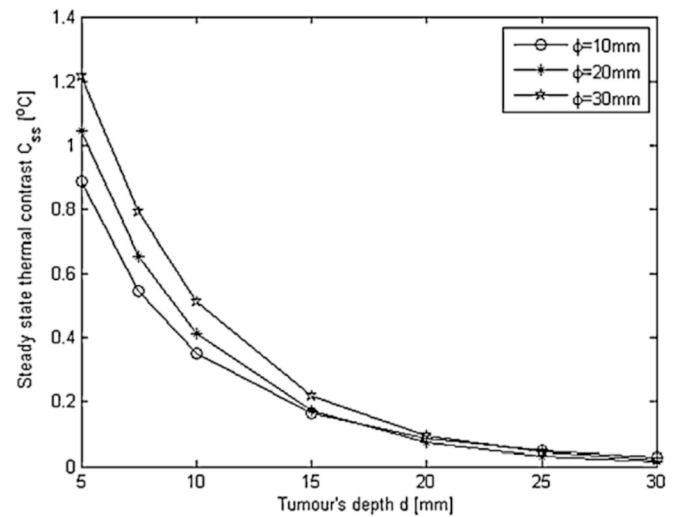


Fig. 1. Steady state thermal contrast as a function of tumor diameter and depth [82].

detection of breast cancer. To estimate the extent to which thermal contrast can be enhanced, the penetration depth of cold stress is calculated. The penetration depth (δ) is determined as the length in the direction perpendicular to the surface at which the temperature is equal to $0.99T_i$ and can be defined as a function of thermal diffusivity (α) and time (t) [92]:

$$\delta = 3.65\sqrt{\alpha t} \quad (1)$$

Thermal diffusivity is determined by the equation of transient conduction equation in one dimension [92]:

$$\frac{\partial^2 T(x, t)}{\partial x^2} = \frac{1}{\alpha} \frac{\partial T(x, t)}{\partial t} \quad (2)$$

where T is the temperature, x is length in the direction normal to surface, t is the time; α is the thermal diffusivity. At the condition when: $T(x=0; t>0) = T_0$; $T(x \rightarrow \infty; t>0) = T_i$; $T(x>0, t=0) = T_i$, where T_0 is the temperature of the cold stress; T_i is the temperature of the tissue.

According to Gonzalez-Hernandez et al [92], the thermal diffusivity of the glandular tissue is equal to $1.52 \times 10^{-7} \text{ m}^2/\text{s}$ (Fig. 2b). Therefore, for the tumors at a depth less than 20 mm, the time of applying cold stress equals to about 4 min, whereas for the tumors at the depth of more than 30 mm this time is more than 9 min.

According to the study by Chanmugam et al [93], the depth of penetration varied with the duration of cold stress. For a duration of 2 min, the penetration depth was 6 mm measured at points along the axis, considering a temperature decrease of 0.3 °C, which is consistent with the temperature under the same steady state conditions. The authors noted that the most frequently observed temperature difference between healthy and cancerous tissue occurred between 10 and 20 min after cold exposure. Moreover, the study by Amri et al [82] showed that for the

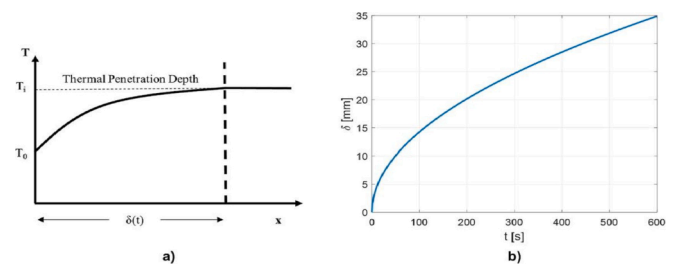


Fig. 2. Penetration depth: (a) schematic representation; (b) function of time [92].

same depth of 20 mm, the estimated time for cold stress was 2 min at a cooling temperature of 15 °C. This cooling time is sufficient to achieve the maximum thermal contrast. However, for tumors deeper than 20 mm, this cooling time is not sufficient because a longer observation and cooling time is required.

In contrast, Ng and Sudharsan [77] analyzed the effect of cold stress on temperature distribution and rewarming process. In the study, numerical calculations were performed for the cases of 1, 3 and 5 min application of cold stress. The results of the study showed a temperature increase between 0.05 and 0.045 in non-dimensional terms; such thermal contrast does not provide valuable information about the temperature pattern. Observing the warm-up process of 60 min, the authors determined a thermal contrast of 0.16 °C and concluded, following the study of Usuki et al [47], that such a thermal contrast is sufficient to clearly identify the abnormality. In addition, another study by Jiang et al [54] concluded that to achieve the required thermal contrast, the minimum cooling time should be 25 min at a cooling temperature below 15 °C, which was not possible due to the extremely uncomfortable conditions for the patients. Therefore, transient numerical simulations were performed to find ways to increase the thermal contrast between healthy and cancerous tissues. However, the results of most of these studies were not practical. The reason is either that the simulated breast areas do not correspond to the real ones, or that the structures of the numerical breasts do not reflect the real ones. In addition, the boundary conditions of the studies also did not match the real conditions. In this regard, it is better to simulate convection around the breast because of the cooling of the breast, and thus achieve higher accuracy in tumor detection.

Detection of abnormalities in thermograms is not only for diagnosis, but also for obtaining detailed patient-specific information about the tumor, such as the size, depth, heat generation or blood perfusion, which can be performed as an inverse problem. This is a different type of problem, especially considering that there may be different combinations of tumor sizes and positions for a thermogram [74,75].

Inverse modeling is the evaluation of the uncertain model parameters when the solution is identified (Fig. 3). In breast cancer detection using thermography, the surface thermogram obtained is one of the solutions to the bioheat equation. To perform inverse thermal modeling, several steps are required: 1) create a computational breast domain (Section 3.2); 2) set the boundary conditions for the selected bioheat equation; 3) apply one of the optimization tools to find the correct parameters; 4) solve the bioheat equation and evaluate the newly obtained solution; 5) repeat steps 3) and 4) until the appropriate parameters are found. The goal of inverse modeling is to find the correct parameters so that the solution matches the temperature distribution of the input surface provided by the thermogram. The most commonly used tools for optimization are: Levenberg-Marguardt algorithm, Genetic Algorithm

and Gradient Descent Method.

The Levenberg-Marguardt (LM) algorithm was used in two studies by Jiang et al [94] and Hatwar and Herman [95]. Jiang et al [94] used the LM algorithm with the primary thermal parameters and developed an inverse method to evaluate the tissue thermal parameters based on the temperature distribution on the breast surface. To evaluate the normalized thermal parameters, the authors investigated iterative nonlinear optimization (Fig. 4a). The results of the inverse modeling for tumor sizes of 8 and 16 mm showed an improvement in tumor detectability regardless of tumor depth. The correlation coefficient for tumor detection had values almost equal to 1. Hatwar and Herman [95] implemented the scheme shown in Fig. 4b. The authors argued that the steady state data were insufficient to estimate three parameters (location, size, and blood perfusion) simultaneously. Therefore, the authors included transient modeling to accurately estimate tumor location and size, and then attempted to include blood perfusion assessment. For the inverse reconstruction, the authors used a LM algorithm (Fig. 4b) that uses the temperature distribution on the skin surface to characterize the tumor. Tumor parameters with the following ranges were used in the study: 12 mm to 30 mm depth, 7 mm to 11 mm radius, and blood perfusion rate from 0.003 l/s to 0.01 l/s. The results showed that the detection accuracy decreased as the depth of the tumors increased. The tumors with blood flow rate of 0.01 l/s and radius of 11 mm showed high accuracy when they were at a depth of 20 mm from the body surface. Thus, the method has proven to be effective, but it can be further improved by using computed tomography images (CT) and improving the accuracy of perfusion in large tumors.

There are several studies using Genetic Algorithm (GA) and Artificial Neural Network (ANN) or curve fitting method to assess tumor size, location, and metabolic heat. Mital and Pidaparti [96] first used ANN to map the thermograms obtained and then used GA to determine the tumor parameters such as size, location and metabolic heat evolution rate (Fig. 5a). The study showed good accuracy of the results for the 2D cases studied. However, the 2D geometry is not an accurate representation of the real breast. In reality, the breast has a complex 3D geometry and structure, so the study should be further improved in terms of geometric representation of the breast. Das and Mishra [80,81] used GA, to simultaneously evaluate the characteristics of the breast and the tumor inside based on the temperature distribution patterns (Fig. 5b). The authors used the curve fitting method (CFM) to estimate the size and location of the tumor and concluded that CFM is a less time consuming tool compared to GA. In the authors' first study, 1D and 2D geometries of the breast were used. However, it was found that these results did not reflect the actual geometry, so the study was extended to 3D geometries of the breast. The results of the CFM method were in agreement with the Gaussian distribution. Considering the predefined accuracy of $\pm 0.75\%$, the method was able to accurately detect tumors with a diameter of at least 3 mm. However, as the depth of the tumor increased or the size of the tumor decreased, the detection of the tumor in the breast based on the temperature distribution became increasingly inaccurate. A study by Mitra and Balaji [97] also used the ANN as in one of the studies by Mital and Pidaparti [96] to estimate the size, depth and metabolic heat generation of the tumor. However, compared to the previous study, this work used steady-state data and a single-layer 3D breast model. Paruch et al [98] also used GA with the gradient method (GM) to estimate tumor size and location. The accuracy of the method (highest error) was calculated to be 0.79% for the thermal parameter assessment of GA and 7.5% for the geometric parameters estimated by GM.

Another technique used in inverse modeling to find the parameters of the tumor based on the so-called inverse heat conduction problem (IHCP) was sequential quadratic programming (SQP), an iterative gradient-based method (IGBM). This method was explored by Bezerra et al [79] to determine the thermal conductivity and blood flow of breast tissue based on an IHCP scheme. The results showed that the thermal properties could be determined based on the extreme temperature points of the thermogram, with a maximum error of 1.28%. However,

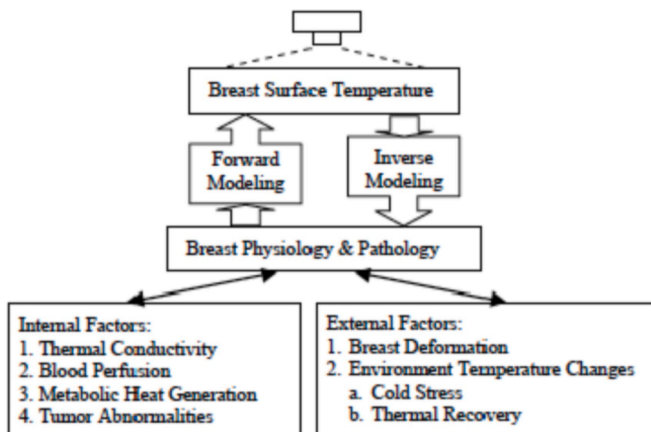


Fig. 3. Diagram of thermal direct/forward and inverse modeling [94].

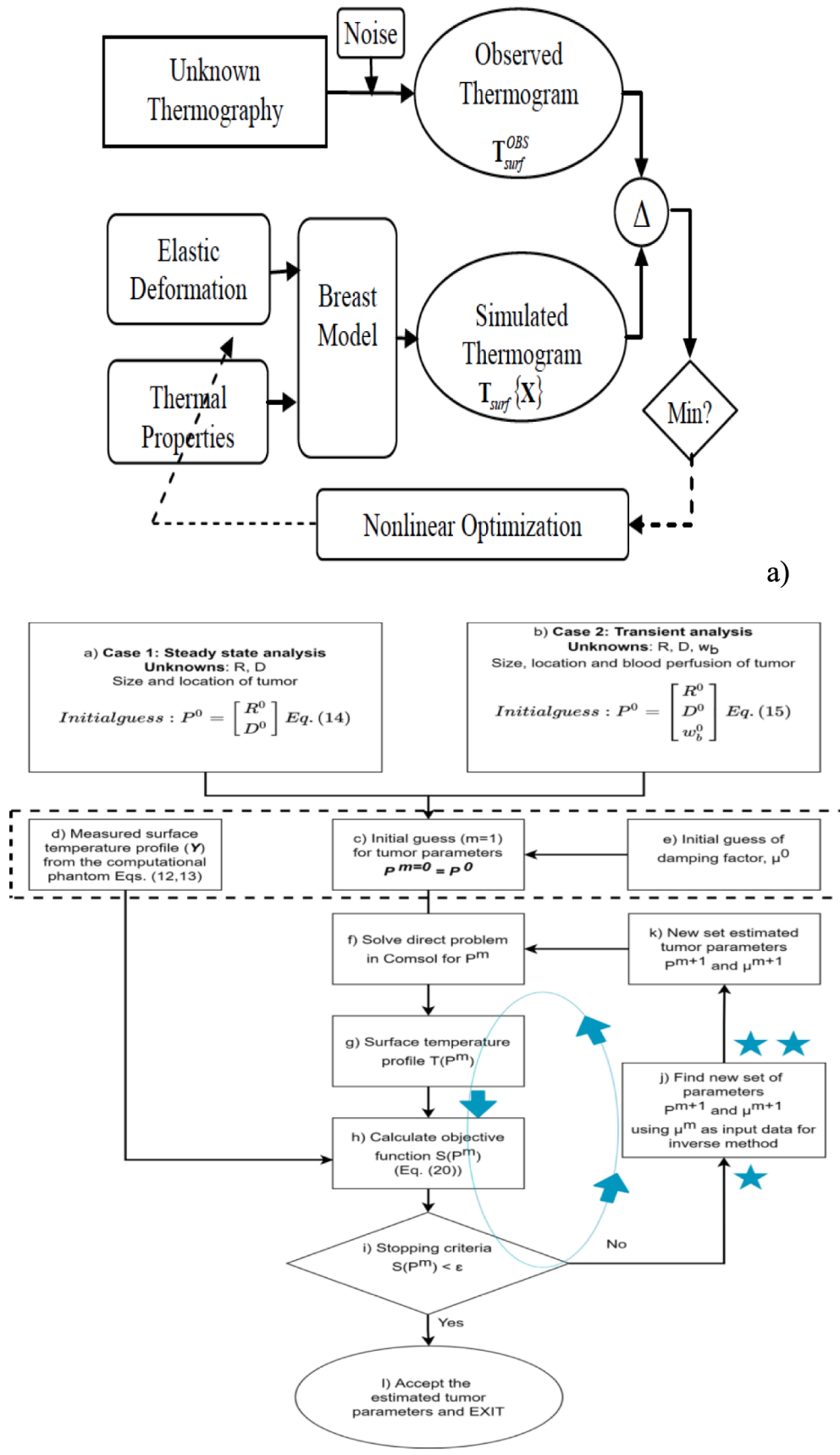


Fig. 4. Flowchart showing inverse reconstruction algorithm for the studies: a) [94]; b) [95].

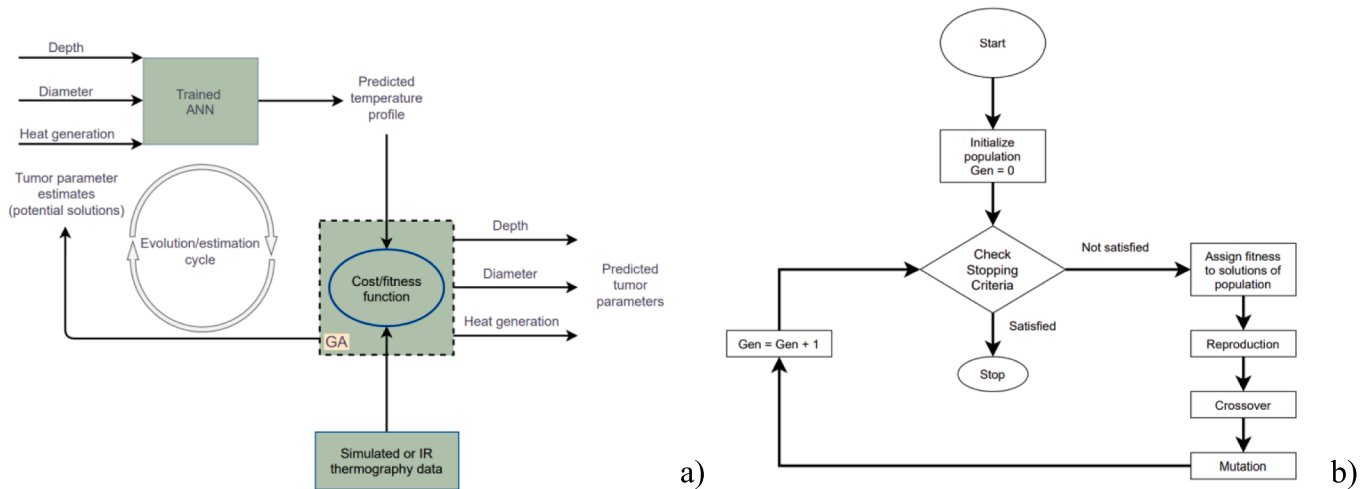


Fig. 5. Flowchart showing the steps of the inverse thermal modeling using GA: a) and ANN in [96] b) and curve fitting method in [80].

according to the authors, further improvements are needed, especially in senior women, and additional layers should be considered in 3D breast models. In addition, other methods such as the second-order Finite Difference -scheme with a pattern search algorithm [99,100], the boundary element method with the simulated annealing technique [101], and MATLAB algorithms [102] could be applied to determine the thermal properties of the breast tissue as well as the parameters of the tumor and the geometric properties of the breast.

It can be concluded that inverse modeling proves to be feasible and consistent to simultaneously determine patient-specific tumor and tissue parameters based on breast geometry and thermograms. The main limitation of the studies performed is the lack of thermograms and breast geometries to validate the obtained results and develop sustainable methods. Therefore, thermography can be further improved by developing intelligent thermogram-based systems using more patient-specific data/information, artificial intelligence and machine learning techniques.

4. From computer-aided diagnosis (CAD) system towards intelligent thermogram-based CAD systems

4.1. Computer-aided thermogram-based diagnostic system

There have been many studies on improving IR imaging as a prognostic adjunctive tool for early detection of breast cancer, and the trend for future research seems to be in computer-aided diagnosis (CAD). A CAD system includes components such as: digital image processing, artificial intelligence, personalized data and physical modeling, and machine detection of temperature distribution patterns. The main advantages of CAD systems are: 1) it is less dependent on human subjective opinion; 2) it is a quantitative based system that can reduce false positives or false negatives; 3) it reduces the cost of additional medical procedures; 4) the system could be automated.

The development of thermography into a complete system CAD involves many steps [45,103–105]: 1) image acquisition and elimination of noise without losing important details; 2) segmentation of the region of interest (ROI); 3) selection and extraction of thermogram features; 4) organization of selected features in databases; 5) characterization and classification of tumors according to the probability of malignancy and any abnormalities; 6) Data mining using machine learning technologies (MLT) [106,107], including K-nearest neighbors (K-NN) [108], ANN [109,110], Decision Tree (DT) [111,112], Support Vector Machine (SVM) [113,114] and Bayesian Networks (BN) [139–146].

The most important development in an intelligent CAD system is the

segmentation of ROI and the subsequent selection and extraction of the data. Therefore, a number of studies have been conducted to improve the approach to understanding and distinguishing features of healthy and tumorous breasts. One of the first studies that focused on facilitating the comparison process was the study by Lipari and Head [115], who segmented the thermograms into different quadrants so that temperature differences between contralateral breasts were more visible. To eliminate diagnostic errors due to human interpretation, the work was extended to automatically compare the temperature profiles of the contralateral breasts [116]. Their results showed that the accuracy of the system can be improved by comparing the statistical analysis of the whole breast with the data obtained from different quadrants. Another work by Qi and Head [117] and Kuruganti and Qi [118] also investigated the automatic selection and extraction of specific features of the healthy and diseased breast from thermograms. The authors proposed to implement this by pixel distributions in accordance with different quadrants into which two breasts were divided.

While some studies aimed to improve image processing and segmentation, others sought to eliminate the influence of human error in diagnosis. One such study, conducted by Irvine [119], investigated automatic target recognition as a tool that could be used to eliminate human error in the diagnosis of breast tumors. In further work by Jakubowska et al [120] and Wang et al [121], an automated thermal image comparison system was developed with the main goal of understanding the differences in thermal properties between breasts with and without malignant tumors. In the field of segmentation, there is another work by Schaefer [122], who used statistical tools together with a fuzzy rule-based classification system to diagnose patients and achieved 80% accuracy in the study. In [123], the authors studied the horizontal and vertical projection profiles to segment two breasts. Morais et al [124] investigated the possibility of using a structured approach to detect abnormal changes in the breast based on thermography. The method used conjugate gradients to compare the measured dimensionless temperature differences between two symmetrical regions of a person's breasts, taking into account the bilateral symmetry of the human body and the environmental conditions. The method was able to detect 96% of breast lesions. The results show that the thermography-based system can be used as a simple, inexpensive, and noninvasive mass screening tool for the early detection of breast cancer. Further studies in the field of breast cancer detection using thermography also aimed to facilitate the process of feature extraction and classification. In this context, the work of Pramanik et al [10] should be highlighted, as a pioneer of a feature extraction method to capture the edges and valleys of thermal breast images for texture analysis and then classify them using a feed-

forward artificial neural network. The detection rate of true-positive images was 100% and false-positive images was 0. Another study that developed a methodology for automatic segmentation of breast images was proposed by Garduno-Roman et al in [11]. The authors used Otsu's method for automatic segmentation of thermograms and also investigated watershed approaches to distinguish abnormal regions of the breasts. The methodology was validated using the Mastology Research database, and 454 cases were tested using the developed methodology. The established method showed a sensitivity and specificity of 0.8684 and 0.8943, respectively, and a segmentation accuracy of 90.3%. The authors of the above studies agreed that thermography in combination with the automated systems of CAD can be used as a supportive and complementary tool for early detection of breast cancer.

Although some developments have been made in CAD systems based on IR thermography, there are still many areas that need improvement. These areas include: 1) automation of CAD systems [115,122,123]; 2) display and processing of thermal images. This is crucial to further improve the efficiency of CAD systems. Currently, thermal images and breast geometries are displayed separately in different formats. Therefore, the correlation between 2D thermal characteristics and 3D breast characteristics may be limited. This area needs further research and improvement; 3) feature extraction and classification methods. These are the core of automatic prediction support. Effective features can be used to identify and automatically remove unwanted regions. Features would also support classification and pave the way for repositories and intelligent diagnosis. This is a critical area for the development of systems from CAD.

In addition, it is envisaged that thermography-based CAD systems will complement, but not replace, mammography. According to the above mentioned studies, thermography-based CAD systems can identify suspicious cases so that these cases can be referred for more detailed mammography and biopsy examinations. In addition, because thermography is non-invasive, more frequent readings can be taken, allowing for more accurate diagnosis through continuous breast temperature measurement. With modern internet facilities and the advancement of 5G internet facilities, data can be updated instantly to ensure timely intervention. Therefore, thermography-based tele-CAD systems have great potential to facilitate mass surveillance of breast cancer in remote areas where medical equipment may not be available.

4.2. Application of artificial neural networks (ANNs) in breast cancer detection

Early detection of breast cancer by IR imaging can be improved by integrating the tool with other approaches. Artificial Intelligence (AI) is considered as a group of algorithms that can explore features of data, and most AI algorithms used for breast cancer detection are mainly related to classification. The goal of such algorithms is to distinguish healthy breasts from those with malignant tumors. They need to be trained with thermographic images of both healthy and malignant breasts [1]. The most useful application of AI is Machine Learning (ML), which focuses on pattern recognition and computational learning theory of AI. Using ML, algorithms can be developed that can learn from data and establish relationships with statistical and mathematical calculations. There are many ML algorithms such as Naïve Bayes, Support Vector Machine (SVM), Decision Tree (DT), Relevance Vector Machine (RVM) and ANN.

ANN is a widely used analysis tool that helps physicians diagnose patients with breast tumors. ANN represents a biophysiological model of the human brain that attempts to mimic its processes. The main building block of ANN is processing elements that are combined in different architectures by ANN to achieve a range of computational capabilities [1]. For ANN, numerous images with and without breast cancer are provided to feed the input layer and processed in the hidden layers. The output of the hidden layers serves as input to the neurons in the output layer, that subsequently leads to decision making. Due to the capability of the ANN

in providing fast evaluation and precise results this tool is preferable compared to other classifiers [125]. The comparative table of performance evaluation in terms of standard descriptors for breast cancer detection using infrared imaging is presented in Table 4.

Ng and Kee [71] used both ANN and biostatistical approaches to diagnose cancer tumors from IR thermograms. They analyzed thermograms from 82 patients (including 30 asymptomatic, 48 benign, and 4 malignant) and identified the inputs of the ANN using regression analysis. According to the authors' report, the maximum accuracy in detecting the tumor was 80.95%, while the accuracy of the radial basis neural network in correctly diagnosing the tumor was 75% in the unhealthy population and 90% in the healthy population.

Mital and Pidarati [96] combined the ANN, GA and thermal simulations to relate skin surface temperature to tumor depth and diameter. To predict the distribution of surface temperature, they trained the ANN with tumor features. Then, the obtained surface temperatures were applied to GA to find the appropriate parameters of the tumor based on a layered hemispherical breast. The errors in determining the depth and diameter of the tumor by GA and ANN were within 5 mm and 2 mm, respectively.

In the study [1], a framework for incorporating ANN into thermography was established, four ANNs were developed and examined using hospital data. The results of the study suggest that better trained neural networks and more accurate detection processes, as well as a reduction in conflicting inputs, are impossible without a large population. Using thermal breast samples generated by thermography and numerical simulations as inputs is another possible approach for training the ANN. This may result in a better trained network since the ANN is a good pattern recognizer. A poorly trained network will give inaccurate results, so using numerical inputs can greatly improve training, as changing tumor parameters in a numerical breast model will generate new training data and the number of available cases becomes unlimited by the amount of clinical data. This is considered an advantage of using computer simulations in ANN training. At the same time, the numerical model needs to be validated by clinical data to generate accurate surface temperatures. Finally, a well-trained ANN can be used as an initial screening tool to process thermograms before numerical thermal inverse modeling is used to actually diagnose tumors.

Saniei [84] proposed a method that can be used to estimate tumor depth, size, and metabolic heat evolution rate. A dynamic neural network and surface temperature distribution obtained from thermal images of the breast were used to support the inverse thermal modeling. To validate the approach, a series of cases with different tumor depths and sizes were studied. As a first step, a finite element thermal model was created and simulations were performed. Similar thermal models were used as the basis for the inverse modeling step, where surface temperatures were used as input to the models to determine the tumor parameters (depth and size). The research results showed that the estimated error in depth was higher than the estimated error in size. The errors were also larger in the deep-seated tumors than in other cases. The results were in agreement with the actual parameters and provided an opportunity to determine the required parameters from a set of surface temperature data.

Wahab et al [126] proposed to improve ANN for tumor localization by using thermal data obtained from previous work. They used several features from a series of numerical simulations performed using different tissue compositions of breast models. These were fed into the optimized ANN system of 6–8–1 network architecture with a pulse constant of 0.3, an iteration rate of 20,000 and a learning rate of 0.2. The overall accuracy of the test and validation results were 96.33% and 92.89%, respectively. The larger error was probably obtained by a large number of neurons previously selected to increase the training complexity.

In the study by Pramanik et al [10], an automatic method for the analysis of chest thermograms was presented. Their approach consists of three main steps including segmentation of breast regions from the

Table 4

The performance evaluation in terms of standard descriptors for breast cancer detection using infrared imaging.

Authors of the study	Method used in the study	Population of the thermograms	Accuracy rate	Sensitivity	Specificity
Ng and Kee [71]	multi-pronged approach comprising of linear regression, radial basis function network (RBFN) and ROC analysis		80.95 %	100 %	70.6 %
Wahab et al [126]	Artificial neural network (ANN)	240 sets of data from the previous simulation works	performance accuracy of 96.33% to testing data and 92.89% to the validation data	No data	No data
Pramanik et al [10]	block variance (BV), feedforward artificial neural network (FANN) with gradient decent training rule	a dataset of 100 frontal view thermal breast images of DMR (Database for Mastology Research)	90 %	95 %	85 %
Acharya et al [130]	Support vector machine (SVM)	50 IR thermograms	85 %	85.71 %	90.48 %
Tan et al [131, 132]	Back propagation algorithm (BPA) Probabilistic Neural Network (PNN) Fuzzy Gaussian Mixture model (GMM) Support vector machine (SVM)	90 patients; 6,000 temperature datasets	83.1 % 86.1 % 77.4 % 90.6 % 85.6 %	82.9 % 88.8 % 78 % 94.8 % 84 %	83.6 % 78 % 75.6 % 78 % 90.4 %
Gayathri Sumathi [133]	Relevance Vector Machine (RVM)	300 dataset	97 %	98 %	98 %
Gogoi et al [134]	The support vector machine (SVM) with radial basis function (RBF) kernel has been used for classification of thermograms	breast thermogram dataset of 60 female subjects	83.22 %	85.56 %	73.23 %
Tcheimegni [135]	SVM	Number of sample 699 (Wisconsin database)	65.52 %	No data	100 %
Rana [137]	RVM		65.52%	No data	100 %
	SVM-linear	UCI depository (WDBC and WPBC)	80.58 %	No data	No data
	SVM-RBF-static 'C' parameter		64.03 %		
	SVM-RBF-dynamic parameter		93 %		
	Logistic regression – generalized		90 %		
	Logistic-regression regularized		92.08 %		
	k-NN-Euclidean		95.68 %		
	k-NN-Manhattan		94.96 %		
	Naïve Bayes-normal		92.1 %		
	Naïve Bayes-kernel		92.1 %		
Nguyen et al [138]	Machine learning method based on random forest classifier and feature selection technique	Wisconsin Database	99.82 %	99.83 %	99.72 %
Silva et al [139]	10-fold cross validation	100 samples	95.38 %	95.37 %	95.37 %
	Leave-One-out cross validation		95.38 %	95.37 %	95.37 %

original images, feature extraction, and classification and performance analysis by using ANN. The background region was removed in the segmentation stage by applying the Otsu thresholding method, followed by a reconstruction method. Finally, the feed-forward ANN with gradient descent training rule was used as a classifier. The main problem of the study was the limited collection of freely available breast thermometer databases. The authors studied 306 breast thermograms of 102 patients obtained from the website Visual Lab [127]. The accuracy, sensitivity and specificity obtained with the proposed system were 90.48%, 87.6% and 89.73%, respectively.

Thus, the studied articles show a high accuracy of ANN in combination with other approaches to diagnose breast tumors. The results of the studies are in agreement with the actual parameters and thus provide an opportunity to determine the required parameters from a group of surface temperature data. Merging ANN, GA, and computer simulations relating breast surface temperature to tumor depth and diameter and heat generation, considering the breast as a computational domain, may offer further improvements in diagnosis. Therefore, ANN, GA and computer simulations can be further investigated to develop an intelligent system for breast cancer detection.

In recent years, Physics Informed Neural Network (PINN) [128,129] has emerged as a hot research topic for solving heat transfer and flow problems as an arbitrary hybrid data and physics-driven simulation method because it uses both the residuals of the underlying differential equations based on physical laws and input data in the loss function for NN (Neural Network) training. This means that PINN can use arbitrary data sets and incorporate more physics into the machine learning process (ML), which helps overcome the limitations of traditional ML methods in finding solutions. For example, thermograms and 3D scans of

the breast can be submitted to PINN as input data, while the heat transfer equations inside the breast and the Navier Stokes equations for airflow outside the breast can be used to train ANNs to simultaneously predict heat transfer and fluid flow, as well as patient-specific tissue properties and tumor size and location. PINN is expected to be the next generation analysis and diagnostic tool that combines the best of physics-based and data-driven simulation.

4.3. Application of different machine learning techniques for breast cancer diagnosis

SVM is one of the discriminatory classifiers commonly used in breast cancer diagnosis. SVM is formally characterized by a separating hyperplane. The comparative table of performance evaluation in terms of standard descriptors for breast cancer detection using IR imaging is presented in Table 4.

One of the first studies on SVMs was done by Acharya et al [130], which they used to classify 50 IR thermograms of breasts, including 25 breasts with a cancerous tumor and 25 normal breasts. Various statistical indicators such as mean, homogeneity, energy and entropy of the thermograms were extracted by the authors. The use of SVM resulted in a specificity of 90.48% and sensitivity of 85.71%. The sensitivity is higher than the typical sensitivity of 78% achieved by a radiologist. Although the results obtained by the authors are promising, the number of tests and the size of the database they used for training were too small. Therefore, it is impossible to generalize these results.

Tan et al [131,132] employed 5 different classifiers including feed forward and probabilistic neural networks, fuzzy classifiers, Gaussian mixed models and SVM. 6000 temperature datasets were collected from

16 thermocouples placed on the patients' breasts (16 thermocouples per patient or 8 on each breast). The author used 5000 and 1000 data for training and testing the classifiers respectively for research purposes. The specificities achieved by all classifiers were above 80%. The SVM showed the best performance with an average accuracy of 90.4% [131].

Gayathri and Sumathi [133] employed a RVM for breast cancer detection by creating a user-friendly environment for its diagnosis. In their study, the authors compared RVM with SVM, and the former method showed better results than the latter. The study showed the differences between the variables and their accuracy, which was not very high, as the accuracy was up to 96%.

The study by Gogoi et al [134] aimed to evaluate the effectiveness of the highly sensitive Infrared Breast Thermography (IBT) in the early diagnosis of breast abnormalities. Their study investigated the effectiveness of IBT by performing temperature-based analysis (TBA), intensity-based analysis (IBA), and Tumor location matching (TLM). To discriminate healthy, malignant and benign breast thermograms in TBA and IBA, a set of temperature and intensity features were retrieved from each thermogram, from which thirteen different sets of features were then determined. Their classification performance was evaluated using SVM with radial basis function kernel. Among all the feature sets, the one that contained statistically significant ($p < 0.05$) features provided the highest classification accuracy of 83.22% with 73.23% specificity and 85.56% sensitivity. The results of the study indicate that IBT can be used as a proactive method for early detection of breast abnormalities in asymptomatic population.

Tcheimegni [135] used a kernel-based RVM to classify cancers. In this study, the author developed a hierarchical Bayesian model with a sigmoid kernel and a radial basis function (RBF). The author also attempted to classify various diseases based on clinical data using the data-driven model. When comparing RVM and SVM, the author found that RVM has better accuracy than SVM of more than 90%.

Bharathi and Natarajan [136] performed classification of cancer using SVM and RVM based on the model ANOVA. The core of their research was to select the smallest genes from microarray data to classify cancer effectively. The ANOVA was used for feature selection. The selection was based on a ranking scheme. The selected genes were introduced into SVM and RVM, where RVM showed higher accuracy of more than 93%.

Rana et al [137] conducted a comparative study using different machine learning methods such as SVM, logistic regression (LR), KNN and Naïve Bayes for detecting breast cancer and predicting its recurrence. The accuracy of the results for the diagnosis of breast cancer was 95.6% and for the prediction of breast cancer recurrence and non-recurrence was 68%.

Nguyen et al [138] developed a computer-aided detection system to classify benign and malignant tumors. They used the backward elimination approach (BE) along with the random forest tree method for feature selection, which consisted of a total of 33 variables and then reduced to 17–18 variables. The accuracy of this hybridized algorithm has been shown to be 99%.

Silva et al [139] conducted a study proposing a hybrid methodology of supervised and unsupervised machine learning to investigate dynamic infrared thermography for diagnosing patients with breast cancer. Dynamic infrared thermography was used to quantitatively measure or monitor the temperature changes on the breast surface after thermal stress. The test results confirmed the diagnostic ability of the proposed method for patients with breast cancer. It should be noted that the classification algorithms such as K-Star and Bayes Net had a classification accuracy of 100% for 39 cases tested. Moreover, the accuracy of classification algorithms such as Bayes Net, Multilayer Perceptron, Decision Table and Random Forest was 95.38%. The proposed approach was able to detect patients with potential cancer regardless of the location of the disease in the breast, but did not allow determination of the location of the abnormality in the breast.

Thus, the abovementioned studies agreed that SVM has high

performance evaluation characteristics compare to other classifiers. However the indicators are not high enough to recommend the proposed approaches as standalone tool for breast cancer detection. At the same time some of the methods could be used as supplementary tool together with other gold standard methods as mammography, ultrasound and MRI.

4.4. Detection of breast cancer using thermographic data and Bayesian networks

Sometimes there is a misunderstanding and confusion about the value and wide applicability of Bayesian networks (BNs). One of the reasons for confusion is that BNs can be used for both unsupervised/supervised learning (and so they sound similar although they are very different to ANNs) and for decision making encapsulating utilities (decision theory). The fundamental potential of BNs is that they comprise a mathematically consistent knowledge representation framework. Therefore the nodes of the network are representing pieces of knowledge that make sense. Mathematically the probabilistic nodes are random variables. Thus, a trained BN can be understandable and readable and also can be used to teach someone. The same is not true for ANNs which are like black boxes. ANNs are better for some tasks like image recognition. In the case of thermography BNs can be used both for predicting the tumor but they can also be used to construct a holistic decision making tool that can drive the correct diagnosis based on information from thermography via Bayes Net and/or via ANNs as well as utilizing other methods. Furthermore, a BN expert model can also encapsulate certain or uncertain knowledge, extra tests, other risk factors or physicians beliefs to make the final diagnosis after thermography.

Bayesian Network Classifiers assign class labels to unlabeled cases, the classification finds a function that associates each unlabeled case to its corresponding label (class). The Naive Bayes classifier (NB) is one successful and popular classifier. A benchmark with respect to it, other classifiers have to be tested. An NB achieves learning from training data samples. Learning in the case of BNs means to construct the conditional probability of each state of variable given the class. NB for a new case, applies Bayes' rule and after selects the value of the class with the highest posterior probability.

The authors in [140] proposed a diagnostic method based on a score formed from thermographic data. 16 variables had been used to calculate this score (they comprise the nodes of the BN). The diagnostic power of the proposed variables was also estimated. 98 cases (21 healthy) had been examined and were used to build a diagnostic model and calculate its accuracy, sensitivity, and specificity.

The authors have applied the BN method with three different types of classifiers and compared this method with other techniques such as ANNs and decision trees. They confirmed that the advantage of BNs was that they permit someone expert/physician visually to determine which factors have an influence over the diagnosis outcome and how variables influence each other. ANNs exhibit similar performance but they lack explanation. They cannot explain how a decision is made and which are the critical variables that influence the diagnosis more. Decision trees have a limited explanation capability, but they cannot encapsulate interactions of explanatory variables. The analysis in [140] reveals poor specificity but very high sensitivity and accuracy. Larger and more balanced thermographic dataset is required.

In [141] the authors studied again with BN networks and various classifiers with the same dataset in [140]. They reconfirmed the results of [140] regarding accuracy sensitivity and specificity. The main conclusion was that the thermographic variables were subjective and should be reconsidered. The analysis with the help of the Bayesian network showed that only 2 out of the 16 variables influenced the diagnosis. A more balanced and larger dataset is needed.

The authors in [140] suggested to use 20 statistical quantities as characteristic variables to extract information from thermographic images. These variables were texture features extracted from the Gray

Level Co-occurrence Matrix (GLCM). This Matrix otherwise called gray level spatial dependence matrix evaluates the spatial relationship of pixels. The GLCM values the texture of the thermography image, estimating how frequent pairs of pixels with certain values and in a given orientation "0" and distance "d" from each other happen in an image. Thus, this paper answers to the subjectivity issues of the variables that have been chosen in papers [140,141].

In [142] the classification of the healthy and unhealthy cases had been done using three different classifiers: SVM, k-NN classifier and NB classifier. In this paper the sample is small 26 normal and 14 abnormal images were studied. ROC analysis showed that the best accuracy was achieved with k-NN classifier. In this work the accuracy achieved was high but the dataset needed to be enlarged for safer conclusions and diagnosis.

In [143] the authors proposed a hybrid methodology using unsupervised and supervised learning techniques. In the previous works [140–147] supervised learning was only utilized. Another difference of this work was that DIT data was used. Therefore the datasets were time series. The IR camera monitored temperature gradients, after a thermal stress. The first step of their method was to perform a clustering by k-means algorithm. Next, classification using BN, NN, decision rules and decision tree was carried out. In this work 40 healthy cases and 40 with cancer cases were considered. The analysis in [143] was quite thorough. The authors executed 39 different classification algorithms. K-Star and Bayes Net outperformed and resulted in 100% accuracy. One drawback of this method is that it cannot determine the location in the breast tumor. Reverse thermal engineering is required for such a task.

In the work in [144] a larger set of thermographic data had been used. 1052 images were analysed. Another improvement that this paper introduced was that the images were classified into malign, benign, cyst and normal groups from specialists and biopsy. Thus, the training and the final diagnosis concerned 4 different states and not just two like in all other reviewed works of this subsection. A third improvement in [144] was that the authors defined as variables attributes based on both geometry and texture. They used the so-called Zernike geometry moment (projections of the image function in orthogonal basis functions) and Haralick texture moment (co-occurrence matrix of the image). The classifiers executed were Bayes Network, NB, SVM, Knowledge Tree J48, Multi-Layer Perceptron (MLP), Random Forest, Random Tree, and Extreme Learning Machines (ELM). The analysis resulted in a fair accuracy with ELM and MLP doing better. However, the BN also provided very good accuracy and much better if the variables in use exhibit independence. It is obvious that in [145] the combination of all these features concerning geometry and texture include variables that are correlated.

Finally, in [146] the authors proposed a method to diagnose normal or abnormal images (with cancer or without). The novelty of this work is the use of the combination curvature function and gradient vector flow method for breast segmentation. Furthermore, in this work the classification analysis used the new powerful type of ANN called convolutional neural networks (CNN). The authors presented in [147] a comparison of CNN with tree random forest (TRF), MLP, and BN. CNN technique outperformed the rest and succeeded with perfect accuracy. The dataset was not that large and had only 73 breast images, but the overall efficiency was very high and CNN was found to have 100% TPR (true positive rate or sensitivity: $TPR = TP/(TP + FN)$), SPC (specificity or true negative rate: $SPC = TN/(TN + FP)$), and ACC (accuracy: $ACC = (TP + TN)/(TP + FP + TN + FN)$).

In summary BN and NN are very strong ML tools but at the same time they are conceptually different. Modern NN in the recent last ten years surprised all researchers with their incomparable ability to recognize patterns. Their applicability to real life AI problems attracted the interest of many investors and companies. However, the way that they find solutions is a black box. BN on the other hand are very useful for medical problems where you want to build an expert model for diagnosis. BN are conceptually different in the sense that they encapsulate the knowledge

from data in variables that can be concepts of a domain expert. Furthermore, this is the only framework that can provide causal reasoning that explores causes and effects.

It is noted that all the works reviewed here concerning breast cancer diagnosis use thermography and BNs for classification only. No researcher utilizes the second big advantage of BNs: their ability to build a holistic expert model that can encapsulate certain and uncertain knowledge from AI classifiers from physicians from other tests etc. A BN expert model can integrate different diagnosis results coming from different AI techniques or other methods and suggest the final decision based on the utility theory.

5. Summary and conclusion

A number of studies were conducted to identify whether thermography could be employed as a reliable tool to detect the breast tumor. Most of the studies agreed that thermography has potentials to be a noninvasive, safe and reliable tool for earlier breast cancer detection and prediction. However, at the present thermography could only be a supplementary tool for mammography, as it is very sensitive to the conditions of the procedure and wellness of the patient. Moreover, the main limitation of thermography is the weak surface signature of small and deep tumors. Notwithstanding, there is a renewed wave of interest in thermography because of the improvement of IR cameras sensors, though the development of such cameras still does not provide a more quantitative and robust procedure to detect the breast tumor.

On the other hand, the improvement of computer systems shows that mathematical modeling can also provide promising opportunities to improve the accuracy and reliability of tumor diagnosis. Numerical modeling of the tumor inside the breast is a complex process, at the same time it is a reliable one to supplement thermography and helps us to shift from qualitative to the quantitative assessment of the thermograms. Nonetheless, numerical methods and models can only be improved by validation against benchmark experimental data. Future research should focus on the development of sophisticated patient-specific models for precision prediction of all the thermal phenomena in the breast, employing personalized or patient-specific characteristics of the breast and its tissues. This can be achieved by carrying out reverse thermal modeling using the healthy and diseased breast thermograms and breast 3D geometry as inputs. Furthermore, these models can be used to improve thermal contrast in the transient cooling with dynamic IR thermography for the breast. It is also suggested that future thermography should contain the 3D distributions of surface temperature using 3D breast geometries. It can further be modified with a multilayer tissue model for improved accuracy and in an effort towards personalized medicine for breast cancer. This level of accuracy is important for revealing the exact correlation between the characteristics of the tumor and its thermal signature.

Artificial intelligence is recognized as an effective tumor classification tool with high sensitivity and specificity. The most useful application of Artificial Intelligence is Machine Learning. There are many Machine Learning algorithms such as: Naïve Bayes, Support Vector Machine, Decision Tree, Relevance Vector Machine, Convolutional Neural Network and Artificial Neural Network. AI techniques show good levels of accuracy, sensitivity and specificity obtained in the conducted studies. However the main limitation of the conducted studies is the limited number of thermograms available to be used in the studies, therefore the low levels of the robustness of the results of the study. It should be noted that these methods are not used in clinics and hospitals, as further developments are required to combine thermography, physics-based modeling and data-driven computation to diagnose breast cancer. Physics Informed Neural Network (PINN) seems to be an ideal method for such integration. Note also, that BNs can be the final layer that encapsulates and integrates in a mathematical consistent way, the knowledge coming from thermal modeling from various medical tests, from patient history profile, from experts and from one or more AI

diagnostic methods/tools towards the final diagnosis decision.

For future studies, it is recommended to have publicly available standardized image databases, which include images from different modalities for similar cases in order to facilitate the tasks of classification based on the machine learning, data-driven simulation and physics-based modeling.

Declaration of Competing Interest

The authors declare that they have no known competing financial interests or personal relationships that could have appeared to influence the work reported in this paper.

Acknowledgement

The authors are grateful to the Ministry of Education and Science of the Republic of Kazakhstan for financing this work through the grant financing under the project “Application of artificial intelligence to complement thermography for breast cancer prediction” (AP08857347) and Nazarbayev University for administering the research project.

References

- [1] *Infrared Imaging technology for breast cancer detection – Current status, protocols and new directions*. S.G. Kandlikar, I. Perez-Raya, P.A. Raghupathi, J.S. Gonzalez-Hernandez, D. Dabdeen, L. Medeiros, P. Phatak. s.l.: International Journal of heat and mass transfer, 2017, Vol. 108, pp. 2303-2320.
- [2] *The causes of cancer: quantitative estimates of avoidable risks of cancer in the United States today*. R. Doll, R. Peto. Cancer, USA: J. Natl. Cancer Inst., 1981, J. Natl. Cancer Inst., Vol. 66(6), pp. 1192-1208.
- [3] *The causes and prevention of cancer*. B.N. Ames, L.S. Gold, W.C. Willett. Cancer, Washington, DC: <https://doi.org/10.1073/pnas.92.12.5258>, 1995, Proc. Natl. Acad. Sci., Vol. 92(12), pp. 5258-5265.
- [4] *Institute, National Cancer*. National Cancer Institute. [Online] NIH Turning Discovery Into Health. [Cited: August 2, 2020.] <https://www.cancer.gov/types/breast/patient/breast-treatment-pdq#section/all>.
- [5] World Health Organization (2021). Breast Cancer. Retrieved from <https://www.who.int/news-room/fact-sheets/detail/breast-cancer>.
- [6] A.B. Mariotto, K. Robin Yabroff, Y. Shao, E.J. Feuer, M.L. Brown, JNCI, J. Natl. Cancer Inst 103 (2) (2011) 117–128.
- [7] *An improved three-dimensional direct numerical modelling and thermal analysis of a female breast with tumour*. E.Y.K. Ng, N.M. Sudharsan. 2001, Proc. Inst. Mech. Eng., Vol. 215 (1), pp. 25-37. 25-37.
- [8] J.R. Keyserlingk, P.D. Ahlgren, E. Yu, N. Belliveau, M. Yassa, IEEE Eng. Med. Biol. Mag. 19 (3) (2000) 30–41.
- [9] *Relationship between microvessel density and thermographic hot areas in breast cancer*. T. Yahara, T. Koga, S. Yoshida, S. Nakagawa, H. Deguchi, K. Shirouzu. 2003, Surg. Today, Vol. 33 (4), pp. 243-248. 243-248.
- [10] *2016 International Conference on Advances in Computing, Communications and Informatics, ICACCI 2016*. S. Pramanik, D. Bhattacharje, M. Nasipuri. 2016. Texture analysis of breast thermogram for differentiation of malignant and benign breast. pp. 8-14.
- [11] *Supportive Noninvasive Tool for the Diagnosis of Breast Cancer Using a Thermographic Camera Sensor*. M.A. Garduno-Ramon, S. G. Vega-Mancilla, L.A. Morales-Henandez, R.A. Osorio-Rios. s.l.: doi:10.3390/s17030497, 2017, Sensors, Vol. 17, p. 497.
- [12] *Breast thermography and cancer risk prediction*. Gautherie M., Gros C.M. 1980, Cancer, Vol. 45, pp. 51-56. 51-56.
- [13] E.Y.K. Ng, Y. Chen, Ung L.J. Med, Computerized breast thermography: Study of image segmentation and temperature cyclic variations, Eng. Technol. 25 (2001) 12–16.
- [14] N. Bjurstam, K. Hedberg, K. Hultborn, N. Johansson, C. Johnsen, Diagnosis of breast carcinoma. In progress in surgery, London: Karger Publishers (1974) 1–65.
- [15] The radiation of heat from the human body. I. An instrument for measuring the radiation and surface temperature of the skin. Hardy, J. D. 1934, J. Clin. Invest., Vol. 13, pp. 593-604.
- [16] “The radiation of heat from the human body. II. A comparison of some methods of measurement,”. Hardy, J. D. 1934, J. Clin. Invest., Vol. 13, pp. 605-614.
- [17] “The radiation of heat from the human body. III. The human skin as a black-body radiator,”. Hardy, J.D. 1934, J. Clin. Invest., 13 615–620 (1934), Vol. 13, pp. 615-620.
- [18] The radiation of heat from the human body. IV. The emission, reflection, and transmission of infrared radiation by the human skin. J. D. Hardy, C. Muschenheim. 1934, J. Clin. Invest., Vol. 13, pp. 817-831.
- [19] *The radiation of heat from the human body. V. The transmission of infra-red radiation through skin*. J. D. Hardy, C. Muschenheim. 1935, J. Clin. Invest., Vol. 14, pp. 1-9.
- [20] Goniometric spectrometer for the measurement of diffuse reflectance and transmittance of skin in the infrared spectral region. C. Clark, R. Vinegar, J. D. Hardy. 1953, J. Opt. Soc. Am., Vol. 43, pp. 993-998.
- [21] *Spectral transmittance and reflectance of excised human skin*. J. D. Hardy, H. T. Hammel, D. Murgatroyd. 1956, J. Appl. Physiol., Vol. 9, pp. 257-264.
- [22] *Automatic recording reflectometer for measuring diffuse reflectance in the visible and infrared regions*. W. L. Derksen, T. I. Monahan, A. J. Lawes. 1957, J. Opt. Soc. Am., Vol. 47, pp. 995-999.
- [23] *Measurement of the total normal emissivity of skin without the need for measuring skin temperature*. D. Mitchell, T. Hodgson, F. R. N. Nabarro. 1967, Phys. Med. Biol., Vol. 12, pp. 359-366.
- [24] *The calculation of the emissivity of cylindrical cavities giving near black-body radiation*. Quinn, T. J. 1967, Br. J. Appl. Phys., Vol. 18, pp. 1105-1113.
- [25] *Wavelength dependence of skin emissivity*. Watmough, D.J. s.l.: Phys. Med. Biol., 1969, Vol. 14, pp. 201-204.
- [26] *Spectral emissivity of skin and pericardium*. Steketee, J. 1973, Phys. Med. Biol., Vol. 18, pp. 686-694.
- [27] *Foundations of thermometry*. T. J. Quinn, J. P. Compton. 1975, Rep. Prog. Phys., Vol. 38, pp. 151-239.
- [28] W.K. Pratt, in: *Digital Image Processing*, John Wiley & Sons, New York, 1978, pp. 1–24.
- [29] *The optics of human skin*. R. R. Anderson, J. A. Parrish. 1981, J. Invest. Dermatol., Vol. 77, pp. 13-19.
- [30] *Implications of surface temperatures in the diagnosis of breast cancer*. Lawson, R. 1956, Can. Med. Assoc. J., Vol. 75 (4), pp. 309-310.
- [31] *Breast cancer and body temperature*. R. Lawson, M.S. Chughtai. 1963, Can. Med. Assoc. J., Vol. 88(2), pp. 68-70.
- [32] *Thermopathology of breast cancer: measurement and analysis in vivo temperature and blood flow*. Gautherie, M. 1980, Ann. N. Y. Acad. Sci., Vol. 335 (1), pp. 383–415.
- [33] *Thermographic localization of incompetent perforating veins in the leg*. K.D. Patil, J. R. Williams, K.L. Williams. 1970, Br. Med. J., Vol. 1 (5690), pp. 195-197.
- [34] *Detection of breast cancer by liquid crystal thermography. A preliminary report*. T.W. Davison, K.L. Ewing, J. Ferguson, M. Chapman, A. Chan, C.C. Voorhis. 1972, Cancer, Vol. 29 (5), pp. 1123-1132.
- [35] *On the feasibility of obtaining three dimensional information from thermographic measurements*. M.M. Chen, C.O. Pederson, J.C. Chato. 1977, Journal of Biomechanical Engineering, pp. 58-64.
- [36] *An analytical model of the countercurrent heat exchange phenomena*. J.W. Mitchell, G.E. Myers. 1968, Biophys. J., Vol. 8, pp. 897-911.
- [37] *Breast thermography after four years and 10,000 studies*. J.H. Isard, W. Becker, R. Shilo, B.J. Ostrum. 1972, American Journal of Roentgenology and Nuclear Medicine, Vol. 115(4), pp. 811-821.
- [38] O.T. Siu, W.R. Ghent, B.T. Colwell, J.C. Henderson, Thermogram aided clinical examination of the breast – an Alternative to Mammography for women 50 and younger, Canadian Journal of Public Health 73 (4) (1982) 232–235.
- [39] K H Keller, L Seiler, An analysis of peripheral heat transfer in man, J. Appl. Physiol. 30 (5) (1971) 779–786.
- [40] Michael M. Chen, Kenneth R. Holmes, Microvascular contributions in tissue heat transfer, Ann. N.Y. Acad. Sci. 335 (1 Thermal Chara) (1980) 137–150.
- [41] *Heat transfer of blood vessels*. Chato, J. 1980, J. Biomech. Eng.-Trans. ASME, Vol. 102(2), pp. 110-118.
- [42] *Temperature and blood flow patterns in breast cancer during natural evolution and following radiotherapy*. Gautherie, M. 1982, Biomedical Thermology, pp. 21-64.
- [43] *Indirect signs of breast cancer: Angiogenesis Study*. Gamagami, P. s.l.: Atlas Mammogr, 1996.
- [44] *Thermobiological assessment of benign and malignant breast diseases*. Gautherie, M. 1983, Am. J. Obstet. Gynecol., Vol. 147(8), pp. 861-869.
- [45] *A review of thermography as promising non-invasive detection modality for breast tumors*. Ng, E.Y.K. 2009, Int. J. Therm. Sci., Vol. 48(5), pp. 849-859.
- [46] *Analysis of transient thermal processes for improved visualization of breast cancer using IR imaging*. M. Kaczmarek, A. Nowakowski. 2003, Proceedings of the 25th Annual International Conference of the IEEE Engineering in Medicine and Biology Society, Vol. 2, pp. 1113-1116.
- [47] *Advantages of subtraction thermography in the diagnosis of breast disease*. H. Usuki, S. Teramoto, S. Komatsubara, S.I. Hirai, T. Misumi, M. Murakami, Y. Onoda, K. Kawashima, K. Kino, K.I. Yamashita, J. Matsubara. 1991, Biomedical Technology, Vol. 11(4), pp. 286-291.
- [48] *Breast Thermal Imaging: The paradigm shift*. Cockburn, W. 1995, Thermologie Oesterreich, Vol. 5, pp. 49-53.
- [49] J. Mooibroek, J. Crezee, J. Lagendijk, Basic of thermal models: thermoradiotherapy and Thermochemotherapy, Springer, Berlin, 1995, pp. 425–433.
- [50] *Analysis of tissue and arterial blood temperatures in the resting human forearm*. Pennes, H.H. 1948, J. Appl. Physiol., Vol. 85(1), pp. 93-122.
- [51] *Influence of blood supply on thermal properties and metabolism of mammary carcinomas*. Gullino, P.M. 1980, Ann. N. Y. Acad. Sciences, Vol. 335, pp. 1-21.
- [52] Y. Ohashi, I. Uchida, Applying dynamic thermography in the diagnosis of breast cancer. IEEE Eng. Med. Biol. Mag 19 (3) (2000) 42–51.
- [53] C. Herman, The role of dynamic infrared imaging in melanoma diagnosis, Expert Rev. Dermatol. 8 (2) (2013) 177–184.
- [54] L. Jiang, W. Zhan, M.H. Loew, Modeling static and dynamic thermography of the human breast under elastic deformation, Phys. Med. Biol. 56 (1) (2011) 187.
- [55] L. Hu, A. Gupta, J.P. Gore, L.X. Xu, Effect of forced convection on the skin thermal expression of breast cancer, J. Biomech. Eng. 126 (2) (2004) 204.

- [56] *Breast thermography. A prognostic indicator for breast cancer survival.* J.H. Isard, C. J. Sweitzer, G.R. Edelstien. 1988, Cancer, Vol. 62, pp. 484-488.
- [57] *Breast thermography is a noninvasive prognostic procedure that predicts tumor growth rate in breast cancer patients.* J.F. Head, F. Wang, R.L. Elliott. 1993, Ann. N. Y. Acad. Sci., Vol. 698(1), pp. 153-158.
- [58] Anthony J. Guidi, Stuart J. Schnitt, *Angiogenesis in preinvasive lesions of the breast*, Breast J. 2 (6) (1996) 364-369.
- [59] *Comparison of the accuracy of thermography and mammography in the detection of breast cancer.* R. Omranipour, A. Kazemian, S. Alipour, M. Najafi, M. Alidoosti, M. Navid, A. Alikhasshi, N. Ahmadinejad, K. Bagheri, S. Izadi. 2016, Breast Care, Vol. 11(4), pp. 260-264.
- [60] *Administration, U.S. Food and Drug.* U.S. Food and Drug Administration. [Online] [Cited: August 2, 2020.] <https://www.fda.gov/medical-devices/safety-communications/fda-warns-thermography-should-not-be-used-place-mammography-detect-diagnose-or-screen-breast-cancer>.
- [61] W. Wulff, *The energy conservation equation for living tissue*, IEEE Trans. Biomed. Eng. BME 21 (6) (1974) 494-495.
- [62] S. Weinbaum, L.M. Jiji, D.E. Lemons, *Theory and experiment for the effect of vascular microstructure on surface tissue heat transfer. Part I: Anatomical foundation and model*, J. Biomech. Eng. 106 (4) (1984) 321-330.
- [63] S. Weinbaum, L.M. Jiji, D.E. Lemons, *Theory and experiment for the effect of vascular microstructure on surface tissue heat transfer – Part II: Model formulation and solution*, J. Biomech. Eng. 106 (4) (1984) 331-341.
- [64] S. Weinbaum, L.M. Jiji, *A new simplified bioheat equation for the effect of blood flow on local average tissue temperature*, J. Biomech. Eng. Vol. 107 (2) (1985) 131-139.
- [65] M. Zhu, S. Weinbaum, L.M. Jiji, D.E. Lemons, *On the generalization of the Weinbaum-Jiji bioheat equation to microvessels of unequal size; the relation between the near field and local average tissue temperatures*, J. Biomech. Eng. 110 (1) (1988) 74-81.
- [66] S. Weinbaum, L.M. Jiji, *The matching of thermal fields surrounding countercurrent microvessels and the closure approximation in the Weinbaum-Jiji equation*, J. Biomech. Eng. 111 (4) (1989) 271-275.
- [67] *An evaluation of the Weinbaum-Jiji bioheat equation for normal and hyperthermic conditions.* C.K. Charny, S. Weinbaum, R.L. Levin. 1990, J. Biomech. Eng., Vol. 112(1), pp. 80-87.
- [68] S. Weinbaum, L.M. Jiji, D.E. Lemons, *The bleed off perfusion term in the Weinbaum-Jiji bioheat equation*, J. Biomech. Eng. 114 (4) (1992) 539-542.
- [69] S. Weinbaum, L.X. Xu, L. Zhu, A. Ekpene, *A new fundamental bioheat equation for muscle tissue: Part I – Blood perfusion term*, J. Biomech. Eng. 119 (3) (1997) 278-288.
- [70] C. Charny, R. Levin, *Bioheat transfer in a branching countercurrent network during hyperthermia*, J. Biomech. Eng.-Trans. Asme 111 (4) (1989) 413-422.
- [71] E.Y.K. Ng, E.C. Kee, *Advanced integrated technique in breast cancer thermography*, J. Med. Eng. Technol. 32 (2) (2008) 103-114.
- [72] E.Y.K. Ng, N.M. Sudharsan, *Numerical computation as a tool to aid thermographic interpretation*, J. Med. Eng. Technol. 25 (2) (2001) 53-60.
- [73] O. Mukhmetov, D. Igali, Y. Zhao, S.C. Fok, L. Teh, E.Y.K. Ng, A. Mashekova, *Finite element modelling for the detection of breast tumors*, in: Proceedings – 2018 IEEE 18-th International Conference on Bioinformatics and Bioengineering, BIBE, Taichung, Taiwan, 2018, pp. 360-363.
- [74] M.M. Osman, E.M. Afify, ASME, *Thermal modeling of the normal woman's breast*, Journal of Biomechanical Engineering 106 (1984) 123-130.
- [75] M.M. Osman, E.M. Afify, ASME, *Thermal modeling of the malignant woman's breast*, Journal of Biomechanical Engineering 110 (1988) 269-276.
- [76] *Parametric optimization for tumor identification bioheat equation using ANOVA and the Taguchi Method.* N.M. Sudharsan, E.Y.K. Ng. 2000, Proc Instn Mech Engrs, Vols. 214, Part H, pp. 505-512.
- [77] *Effect of blood flow, tumour and cold stress in a female breast: novel time accurate computer simulation.* E.Y.K. Ng, N.M. Sudharsan. 2001, Proc Instn Mech Engrs, Vol. 215 (Part H).
- [78] *Thermal simulation of breast tumors.* Gonzalez, F.J. 2007, REVISTA MEXICANA DE FÍSICA, Vol. 53(4), pp. 323-326.
- [79] *Estimation of breast tumor thermal properties using infrared images.* L.A. Bezerra, M. M. Oliveira, T.L. Rolim, A. Conci, F.G.S. Santos, P.R.M. Lyra, R.C.F. Lima. 2013, Signal Processing, Vol. 93, pp. 2851-2863.
- [80] Koushik Das, Subhash C. Mishra, *Estimation of tumor characteristics in a breast tissue with known skin surface temperature*, J. Therm. Biol. 38 (6) (2013) 311-317.
- [81] K. Das, S.C. Mishra, *Simultaneous estimation of size, radial and angular locations of a malignant tumor in a 3-D human breast – numerical study*, Journal of Thermal Biology 52 (2015) 147-156.
- [82] *Potentialities of steady-state and transient thermography in breast tumour depth detection: a numerical study.* A. Amri, S.H. Pulko, A.J. Wilkinson. 2016, Comput. Methods Programs Biomed., Vol. 123, pp. 68-80.
- [83] *Tumor parameter estimation considering the body geometry by thermography.* Sh. Hossain, F.A. Mohammadi. 2016, Computers in Biology and Medicine, Vol. 76, pp. 80-93.
- [84] Elham Saniei, Saeed Setayeshi, Mohammad Esmaeil Akbari, Mitra Navid, *Parameter estimation of breast tumour using dynamic neural network from thermal pattern*, Journal of Advanced Research 7 (6) (2016) 1045-1055.
- [85] Y. Zhao, A. Mashekova, O. Mukhmetov. *Scientific report. Development of an intellectual system for early detection of breast tumors and prediction of breast cancer development.* Nur-Sultan : National center of science and technology evaluation, 2019. No. APO5130923.
- [86] N.M. SUDHARSAN, E.Y.K. NG, S.L. TEH, *Comput Methods Biomech, Biomed. Engin.* 2 (3) (1999) 187-199.
- [87] H.W. Huang, C.L. Chan, R.B. Roemer, *Analytical Solutions of Pennes Bioheat Transfer equation with a Blood Vessel*, J. Biomech. Eng 116 (2) (1994) 208-212.
- [88] Haifeng Zhang, Zhang, H, *Physics in Medicine and Biology* 53 (3) (2008) N15-N23.
- [89] Sh. Okajima, H. Manuyama, A. Komiya Takeda, *Dimensionless solutions and general characteristics of bioheat transfer during thermal therapy*, J. 34 (8) (2009) 377-384.
- [90] Praveen Kumar Gupta, Jitendra Singh, K.N. Rai, *Numerical simulation for heat transfer in tissues during thermal therapy*, Journal of Thermal Biology 35 (6) (2010) 295-301.
- [91] A. Amri, A. Saidane, *Thermal analysis of a three-dimensional breast model with embedded tumour using the model with embedded tumour using the transmission line matrix (TLM) method*, Comput. Biol. Med. 41 (2011) 76-86.
- [92] *Technology, application and potential of dynamic breast thermography for the detection of breast cancer.* J.L. Gonzalez-Hernandez, A.N. Recinella, S.G. Kandlikar, D. Dabydeen, L. Medeiros, P. Phatak. 2019, International Journal of Heat and Mass Transfer, Vol. 131, pp. 558-573.
- [93] *International Mechanical Engineering Congress and Exposition.* A. Chanmugam, R. Hatwar, C. Herman. Houston, Texas, USA : ASME 2012 International Mechanical Engineering Congress and Exposition, 2012. Thermal analysis of cancerous breast model. Vol. Volume 2: Biomedical and Biotechnology, pp. 135-143. ISBN: 978-0-7918-4518-9.
- [94] *Medical Imaging 2011: Biomedical Applications in Molecular, Structural, and Functional Imaging.* L. Jiang, W. Zhan, M.H.Loew. [ed.] Robert C. Molthen John B. Weaver. 2011. Toward understanding the complex mechanisms behind breast thermography: an overview for comprehensive numerical study. Vols. 7965, 79650H, p. 187. doi: 10.1117/12.8777839.
- [95] *Inverse method for quantitative characterisation of breast tumour from surface temperature data .* R. Hatwar, C. Herman. 2017, Int. J. Hyperthermia, Vol. 33 (7), pp. 741-757.
- [96] *Breast tumor simulation and parameters estimation using evolutionary algorithms.* M. Mital, R.M. Pidaparti. 2008, Model Simul Eng, Vol. Special Issue, p. 6 pages.
- [97] Subhadeep Mitra, C. Balaji, *A neural network based estimation of tumour parameters from a breast thermogram*, Int J Heat Mass Tran 53 (21-22) (2010) 4714-4727.
- [98] *Identification of tumor region parameters using evolutionary algorithm and multiple reciprocity boundary element method.* M. Parush, E. Majchrzak. 2007, Eng Appl Artif Intell, Vol. 20(5), pp. 647-655.
- [99] *Tumor location and parameter estimation by thermography.* J.P. Agnelli, A.A. Barrea, C.V. Turner. 2011, Math Comput Model, Vols. 53 (7-8), pp. 1527-1534.
- [100] *Shape optimization for tumor location.* J.P. Agnelli, C. Padra, C.V. Tumer. 2011, Comput Math Appl, Vol. 62(11), pp. 4068-4081.
- [101] *Procedure to estimate thermophysical and geometrical parameters of embedded cancerous lesions using thermography.* J.M. Luna, R. Romero-Mendez, A. Hernandez-Guerrero, F. Elizalde-Blancas. 2012, J. Biomech. Eng., Vol. 134(3).
- [102] *Clinical breast cancer analysis with surface fitting in the medical thermal texture maps.* F. Ye, G.L. Shi. 2012, Appl Mech Mater, pp. 263-266.
- [103] *Morphological measurement of localized temperature increases amplitudes in breast infrared thermograms and its clinical application.* X. Tang, H. Ding, Y. Yuan, Q. Wang. 2008, Biomed. Signal Process. Control, Vol. 3(4), pp. 312-318.
- [104] Roberta Fusco, Mario Sansone, Salvatore Filice, Guglielmo Carone, Daniela Maria Amato, Carlo Sansone, Antonella Pettrillo, *Pattern recognition approaches for breast cancer DCE-MRI classification: a systematic review*, J. Med. Biol. Eng. 36 (4) (2016) 449-459.
- [105] *Anniversary paper: history and status of CAD and quantitative image analysis: the role of medical physics and AAPM.* M.L. Giger, H.P. Chan, J. Boone. 2008, Med. Phys., Vol. 35(12), pp. 5799-5820.
- [106] *Computer-aided detection/diagnosis of breast cancer in mammography and ultrasound: a review.* A. Jalalian, S.B. Mashohor, H.R. Mahmud, M.I. Saripan, A.R. Ramli, B. Karasfi. 2013, Clin. Imaging, Vol. 37(3), pp. 47-51.
- [107] J. Han, M. Kamber, J. Pei, *Data mining: Concepts and techniques*, Elsevier, Oxford, 2012.
- [108] S.A. Medjahed, T.A. Saadi, A. Benyettou, *Breast cancer diagnosis by using k-nearest neighbors with different distances and classification rules*, Int. J. Com-put. Appl. 62 (1) (2013) 1-5.
- [109] Filippo Amato, Alberto López, Eladia María Peña-Méndez, Petr Vanhara, Aleš Hampel, Josef Havel, *Artificial Neural Networks in Medical Diagnosis*, Journal of Applied Biomedicine 11 (2) (2013) 47-58.
- [110] A. Thakur, V. Mishra, S.K. Jain, *Feed forward artificial neural network: tool for early detection of ovarian cancer*, Sci. Pharm 79 (3) (2011) 493-506.
- [111] *Classification of breast cancer using gene index based fuzzy supervised learning in guest decision tree algorithm.* P. Bethapudi, E.S. Reddy, K.V. Varma., 2015, Int. J. Comput. Appl., Vol. 111(14), pp. 50-57.
- [112] *Proceedings of the Ninth Australasian Data Mining Conference.* M. Shouman, T. Turner, R. Stocker. s.l. : Australian Computer Society, Inc., 2011. Using decision tree for diagnosing heart disease patients. Vol. 121.
- [113] *Hybrid feature selection based weighted least squares twin support vector machine approach for diagnosing breast cancer, hepatitis and diabetes.* D.Tumor, S. Agarwal. 2015, Adv. Artif. Neural Syst., Vol. 2015.
- [114] *The method and efficacy of support vector machine classifiers based on texture features and multi-resolution histogram from 18 F-FDG PET-CT images for the evaluation of mediastinal lymph nodes in patients with lung cancer.* X.Gao, C. Chu, Y.Li, P.Lu, W.Wang, W.Liu, L.Yu. 2015, Eur. J. Radiol., Vol. 84(2), pp. 312-317.

- [115] *Advanced infrared image processing for breast cancer risk assessment*. C.A. Lipari, J. F. Head. Chicago : The 19-th Annual International Conference of the IEEE Engineering in Medicine and Biology Society, 1997. Advanced infrared image processing for breast cancer risk assessment. Vol. 2, pp. 673-676.
- [116] *Computerized image analysis of digitized infrared images of breasts from a scanning infrared image system*. J.F. Head, C.A. Lipari, R.L. Elliot. s.l. : The International Society for Optical Engineering, 1998, Proceedings of SPIE, Vol. 3436, pp. 290-294.
- [117] *Asymmetric analysis using automatic segmentation and classification for breast cancer detection in thermograms*. H. Qi, J.F. Head. s.l. : Proceedings of the 23rd Annual International Conference of the IEEE Engineering in Medicine and Biology Society, 2001. Asymmetric analysis using automatic segmentation and classification for breast cancer detection in thermograms. Vol. 3, pp. 2866-2869.
- [118] *24th Annual Conference and the Annual Fall Meeting of the Biomedical Engineering Society EMBS/BMES Conference*. P.T. Kuruganti, H. Qi. s.l. : Engineering in Medicine and Biology, 2002. Asymmetry analysis in breast cancer detection using thermal infrared images, . Vol. 2, pp. 1155-1156.
- [119] *Targeting breast cancer detection with military technology*. Irvine, J.M. 2002, IEEE Eng. Med. Biol. Mag., Vol. 21(6), pp. 36-40.
- [120] *Thermal signatures for breast cancer screening comparative study*. T. Jakubowska, B. Wiecek, M. Wysocki, C. Drews-Peszyński. 2003. Proceedings of the 25-th Annual International Conference of the IEEE Engineering in Medicine and Biology Society. Vol. 2, pp. 1117-1120.
- [121] Jane Wang, King-Jen Chang, Chin-Yu Chen, Kuo-Liong Chien, Yuh-Show Tsai, Yuh-Ming Wu, Yu-Chuan Teng, Tiffany Ting-Fang Shih, **Thermal signatures for breast cancer screening comparative study**, Biomed. Eng. Online 9 (1) (2010), <https://doi.org/10.1186/1475-925X-9-3>.
- [122] *Thermography based breast cancer analysis using statistical features and fuzzy classification*. G. Schaefer, M. Zawisek, T. Nakashima. 2009, Pattern Recognit., Vol. 42, pp. 1133-1137.
- [123] Dayakshini Dayakshini, Surekha Kamath, Keerthana Prasad, K.V. Rajagopal, Segmentation of breast thermogram images for the detection of breast cancer – A projection profile approach, J. Image Graph 3 (1) (2015), <https://doi.org/10.18178/joig.3.110.18178/joig.3.1.47-51>.
- [124] K.C.C. Morais, J.V.C. Vargas, G.G. Reisemberger, F.N.P. Freitas, S.H. Oliari, M. L. Brioschi, M.H. Louveira, C. Spautz, F.G. Dias, P. Gasperin, V.M. Budel, R.A. G. Cordeiro, A.P.P. Schittini, C.D. Neto, An infrared image based methodology for breast lesions screening, *Infrared Physics & Technology* 76 (2016) 710–721.
- [125] K. Ito, A.W. Asnido, S.A. Daud, E.Y.K. Ng. Thermal analysis on 3D breast cancer model. *Computational modelling and simulation for biomedical applications*. s. l. : Penerbit UTM Press, Vol. Ch 9.
- [126] *Tumor localization in breast thermography with various tissue compositions by using Artificial Neural Network*. A.A. Wahab, M.I. Mohamad Salim, J. Yunus, M.N. Che Aziz. 2015. 2015 IEEE Student conference on Research and Development . pp. 484-488.
- [127] Lab, Visual. Visual Lab. [Online] [Cited: June 7, 2020.] <http://visual.ic.uff.br/en/proeng/>.
- [128] M. Raissi, P. Perdikaris, G.E. Karniadakis, **Physics-informed neural networks: A deep learning framework for solving forward and inverse problems involving nonlinear partial differential equations**, *Journal of Computational Physics* 378 (2019) 686–707.
- [129] **Physics-Informed Neural Networks (PINNs) for Heat Transfer Problems**. S.Z. Cai, Z.C. Wang, S.F. Wang, P. Perdikaris, G.E. Karniadakis. 2021, *Journal of Heat Transfer*. Accepted manuscript posted March 17, 2021. doi:10.1115/1.4050542.
- [130] U. Rajendra Acharya, E.Y.K. Ng, Jen-Hong Tan, S. Vinitha Sree, **Thermography based breast cancer detection using texture features and support vector machine**, *Journal Med Syst* 36 (3) (2012) 1503–1510.
- [131] Comparative study on the use of analytical software to identify the different stages of breast cancer using discrete temperature data. J.M.Y. Tan, E.Y.K Ng, U. R. Acharya, L.G. Keith, J. Holmes. 2008, *J Med Syst*, Vol. 33(2), pp. 141-153.
- [132] An Integrated Index for Breast Cancer Identification using Histogram of Oriented Gradient and Kernel Locality Preserving Projection Features Extracted from thermograms. U. Raghavendra, U.R. Acharya, E.Y.K. Ng, Jen-HongTan, Z. Anjan Gudikar. 2016, *Quantitative Infrared Thermography Journal*, Vol. 13(2), pp. 195-209.
- [133] *Comparative study of relevance vector machine with various machine learning techniques used for detecting breast cancer*. B.M. Gayathi, C.P. Sumathi. 2016 *IEEE International Conference on Computational Intelligence and Computing Research (ICIC)*, 2016, pp. 1-5, doi: 10.1109/ICIC.2016.7919576.
- [134] Usha Rani Gogoi, Gautam Majumdar, Mrinal Kanti Bhowmik, Anjan Kumar Ghosh, **Evaluating the efficiency of infrared breast thermography for early breast cancer risk prediction in asymptomatic population**, *Infrared Physics & Technology* 99 (2019) 201–211.
- [135] E. Tcheimegni., **Kernel based relevance vector machine for cancer classification of diseases**, *Bowie state university* 202 (2013) 630–634.
- [136] A. Bharathi, A.M. Natarajan, **Cancer classification using support vector machines and relevance vector machines based on Analysis of Variance features**, *Journal of computer science* 7 (9) (2011) 1393–1399.
- [137] *Breast cancer diagnosis and recurrence prediction using machine learning techniques*. . M.Rana. 2015, *International journal of research in Engineering and Technology* , Vol. 4 (4), pp. 372-376.
- [138] Cuong Nguyen, Yong Wang, Ha Nam Nguyen, **Random forest classifier combined with feature selection for breast cancer diagnosis and prognostic**, *Journal of Biomedical Science and Engineering* 06 (05) (2013) 551–560.
- [139] *Hybrid analysis for indicating patients with breast cancer using temperature time series*. L.F. Silva, A.A.S.M.D. Santos, R.S. Bravo, A.C. Silva, D.C. Muchaluat-Saade, A. Conci. 2016, *Computer Methods and Programs in Biomedicine*, Vol. 130, pp. 142-153. . doi:10.1016/j.cmpb.2016.03.002.
- [140] C.R. Nicandro, M.M. Efen, A.A. Maria Ysaneli, M.D.C.M. Enrique, A.M. Hector Gabriel, P.C. Nancy, G.H. Alejandro, H.R. Guillermo De Jesus, B.M. Rocio Erandi, . s.l. (Eds.), **Evaluation of the diagnostic power of thermography in breast cancer using Bayesian Network Classifiers**, *Computational and Mathematical Methods in Medicine*, 2013, p. p., <https://doi.org/10.1155/2013/264246>.
- [141] *Assessment of Bayesian Network Classifiers as tools for Discriminating Breast Cancer Pre-Diagnosis based on three diagnostic methods*. M.Y. Ameca-Alducin, N. Cruz-Ramirez, E. mezura-Montes, E. Martin-Del-Campo-Mena, N. Perez-castro, H. G. Acosa-Mesa. s.l. : Lecture notes in computer science (including subseries lecture notes in artificial intelligence and lecture notes in bioinformatics), 2013, Vol. 7269 LNAI. doi:10.1007/978-3-642-37807-2_36.
- [142] M. Milosevic, D. Jankovic, A. Peulic, **Thermography based breast cancer detection using texture features and minimum variance quantization**, *EXCLI Journal* 13 (2014) 1204–1215.
- [143] *The accuracy of digital infrared imaging for breast cancer detection in women undergoing breast biopsy*. G.C. Wishart, M. Campisi, M. Boswell, D. Chapman, V. Shackleton, S. Iddles, A. Hallett, P.D. Britton, 2010, *Eur. J. Surg. Oncol. EJSO* x, Vol. 36 (6), pp. 535-540.
- [144] *Breast Cancer Diagnosis Based on Mammary Thermography and Extreme Learning Machines*. M.A. de Santana, J.M.S. Pereira, F.L. da Silva, N.M. de Lima, F.N. de Sousa, G.M.S. de Arruda, R.C.F. de Lima, W.W.A. de Silva, W.P. dos Santos. s.l. : *Research on Biomedical Engineering*, 2018, Vol. 34(1), pp. 45-53. doi:10.1590/2446-4740.05217.
- [145] *Breast Cancer Identification via Thermography Image Segmentation*. S. Tello-Mijares, F. Woo, F. Flores. 2019. doi:10.1155/2019/9807619.
- [146] *A finite element model of the breast for predicting mechanical deformations during biopsy procedures*. F.S. Azar, D.N. Metaxas, M.D. Schnall. 2000, *IEEE Workshop on Mathematical Methods in Biomedical Image Analysis*, pp. 38-45.
- [147] *Relationship between microvessel density and thermographic hot areas in breast cancer*. T. Yahara, T. Koga, S. Yoshida, S. Nakagawa, H. Deguchi, K. Shirouzu. 2003, *Surg. Today* , Vol. 33 (4), pp. 243-248.